SUPPLEMENTARY MATERIAL

SUPPLEMENTARY METHODS

ANTIBODIES AND REAGENTS

The following antibodies were acquired: anti-p16 (orb228122) and anti-phospho-ERK5 S496 (orb5183) were from Biorbyt, San Francisco, CA. Anti-NRF2 (GTX103322; Gentex, Irvine, CA), anti-thioredoxin (Trx) (14999-1 AP20; Proteintech, Rosemont, IL), anti-p90RSK (MAB 2056; R&D Systems, Minneapolis, MN), and anti-α-tubulin (T5168; Sigma-Aldrich, St. Louis, MO) were also acquired. In addition, antibodies against phospho-ERK5 TEY (3371), ERK5 (3372), phospho-p90RSK (9341), phosphor-p90RSK-Alexa Flour 488 conjugate (13588), p21 (2947), p53 (9282), and anti-poly/mono-ADP ribose (PAR) (83732) were purchased from Cell Signaling Technology (Beverly, MA); anti-CD36 (9156), anti-RSK-1 Alexa Flour 647 conjugate (SC-393147 AF647), and anti-heme oxygenase 1 (SC-10789) from Santa Cruz Biotechnologies (Santa Cruz, CA). Anti-TNFα (NBP1-9532) was purchased from Novus Biologicals (Centennial, CO), anti-Gas6 (BS-7549R) was purchased from Bioss (Woburn, MA), anti-PARP (611039) was purchased from BD Bioscience (San Jose, CA), and anti-gamma H2A.X (ab26350) was purchased from Abcam (Cambridge, MA). Anti-CD14-PE (301806) acquired from Biolegend (San Diego, CA).

Protease inhibitor cocktail (p8340), PMSF (36978), NEM (E3876), paclitaxel (T7402), ifosfamide (I4909), and mitoxantrone hydrochloride (M6545) were purchased from Sigma-Aldrich (St. Louis, MO). Doxorubicin hydrochloride was purchased from (NDC 67457-436-50) Mylan Institutional LLC (Rockford, IL). All cancer drugs were dissolved in DMSO; the final concentration of DMSO in cell culture was 0.1%, which we used as a vehicle control. Each cancer drug concentration used in this study was within the therapeutic range of plasma concentration in humans, as reported previously [1-4], or based on the maximum concentration (Cmax) and the area under the curve data, which are also available from the information on each drug manufacturer's site.

Olaparib (AZD2281) was purchased from Selleck Chemicals (Houston, TX). The lipid profile kit (ab65390), MitoTEMPOL (ab144644), and the ATP assay kit (ab83355) were bought from Abcam (Cambridge, MA), and GM-CSF (415-ML-050/CF) was purchased from R&D Systems (Minneapolis, MN). Seahorse XF Cell Mito Stress Test Kit (103015-100), Seahorse XF Glycolysis Stress Test (103020-100), Seahorse XF Base Medium (103334-100), Seahorse XF24 FluxPak mini (100867-100), and a telomere (TL) PNA kit/FITC flow cytometry kit (K5327) were procured from Agilent Technology (Santa Clara, CA). We also used an ARE reporter kit (60514; BPS Biosciences, San Diego, CA), a chemiluminescence detection reagent kit (NEL105001EA; PerkinElmer, Waltham, MA), an ApopTag peroxidase in situ apoptosis detection kit (S7100; Millipore, Burlington, MA), an efferocytosis kit (4649; Essen Biosciences, Ann Arbor, MI), and an NRF2 activator (492042; Calbiochem, Kenilworth, NJ). Lipofectamine 2000 transfection reagent (11668027), Mitosox Red (M36008), and Vybrant MTT Cell Proliferation Assay Kit (V13154) were purchased from ThermoFisher Scientific (Waltham, MA), and the NAD^+/NADH Assay Kit (MET-5030) was purchased from Cell Biolabs (San Diego, CA).

CONTACT FOR REAGENT AND RESOURCE SHARING

Further information and requests for resources and reagents should be directed to and will be fulfilled by the Lead Contacts, Jun-ichi Abe (jabe@mdanderson.org) or Sivareddy Kotla (skotla@mdanderson.org).

EXPERIMENTAL MODEL AND SUBJECT DETAILS

Generation of ERK5 S496A Mice

Mice containing ERK5 S496A point mutation were generated using the CRISPR/Cas technique. A more detailed method can be found in our recent paper [5]. In short, the sequence CGAGGCUCAGGCGCCUCCAA was used in the variable region of the guide RNA (5 ng/uL) and CTGGCGTTCCTGAGCTGTCACGGGCTTTCGAGGCTCAGGCGCCTCCAGGGGTGCAGCGGG CCCATCTGCAGAAAAGTTGGACAAGGGAAAGGTAATGGCTTACAGATCTG for the donor DNA (15 ng/µL). Cas9 protein was used at a concentration of 50 ng/µL. Pronuclear stage embryos were isolated from previously superovulated and mated C57BL/6N female mice. The embryos were then microinjected with a mixture of CRISPR components using standardized pronuclear injection procedures[5]. Surviving embryos were implanted into day 0.5 pseudopregnant CD-1 females (Charles River Laboratories) either on the day of injection (as one-cell embryos) or the following day (as 2-cell embryos)[6]. PCR was performed on all pups and the PCR products were sequenced to identify the correct point mutation and lack of any additional unwanted mutations surrounding the site of homology-directed repair. The primer pair used for PCR were TCTAGCAGGCTTCGGTCATTGTC and TGCACCTGACACCGTTGATC. For Sanger sequencing of the PCR product, the primer AGGGTGCCATCTCCGACAATAC was used.

Transverse Aorta Coarctation (TAC) Model in Hyper-Lipedema Mice

Eight to 12 week old *Ldlr*$^{-/-}$ mice (LDLR$^{-/-}$: C57BL/6J background (B6.129S7-ldlr^{tm1Her}/J, #002207) were obtained from the Jackson Laboratory (Bar Harbor, ME, USA). Mice were fed an adjusted-calorie high fat diet (HFD) consisting of 21% crude fat, 0.15% cholesterol, and 19.5% casein (cat. no. TD.88137; Envigo, NJ, USA) [7]. Since we did not find a significant difference in the response to radiation and olaparib by sex in IR and TAC-mediated coronary atherosclerosis formation, we used both males and females. The number of mice of each sex in each experiment is indicated in figure legends. The weight range of the mice was 15-25 g. We performed genotyping following the Jackson Laboratory protocol and confirmed that the mice were homozygous. No previous procedures were performed on these mice prior to the experiments in this study.

To induce mouse coronary atherosclerosis, we performed TAC as we had previously described [8]. In brief, pressure overload was induced in mice by constricting the ascending aorta between the innominate and left carotid arteries. Anesthetized mice were placed on a heating pad, and respiration was stabilized by intubation and mechanical ventilation, with a tidal volume of 225 µL at 130 breaths/minutes; anesthesia was maintained via 1.5% (vol/vol) inhaled isofluorane. We performed a left thoracotomy in the second intercostal space. Then we exposed the heart and performed aortic constriction. We used the silk thread with a 27-gauge needle to maintain tightness for performing the aortic constriction. We also performed sham-operation by completing all TAC procedures except that we did not place the silk thread and needle on and tighten around the aorta. We used vicryl-coated 6-0 sutures to close the chest cavity and sutured the skin using a 6-0 nylon thread. After anesthesia was

halted, we waited for the mouse to recover before extubation. An aseptic technique was used throughout the procedure.

All procedures were performed between 9 AM and 5 PM local time in the vivarium designated for animal surgery at MD Anderson. Experimental procedures were approved by the Institutional Animal Care and Use Committee (IACUC, #00001652-RN01). We conducted a double-blind, randomized study; the persons who evaluated the plaque size were blinded until the data analysis was complete.

Mouse Monocyte and Macrophage Culture and Irradiation
Briefly, bone marrow cells were isolated by flushing the femurs and tibias of C57BL/6 wild type mice or various transgenic mice on the C57BL/6 background and differentiated into macrophages by culturing at a density of $1x10^6$ cells/mL in Iscove's Modified Dulbecco's Medium (IMDM) (#13390, Sigma-Aldrich, St. Louis, MO) containing 10% fetal bovine serum (FBS), 10% (v/v) spent medium of L929 cell cultures as the source of macrophage colony-stimulating factor [9], 1% HEPES, and 1% penicillin-streptomycin for 5-8 days at 37 °C and 5% CO_2 in air. Cells were irradiated using the XRAD 320 orthovoltage irradiator (Precision X-Ray, Inc., North Branford, CT), operated at 320 kVp and 12.5 mA at various doses (Gy) at room temperature.

Human Monocyte Culture
Normal human peripheral blood $CD14^+$ monocytes (ATCC PCS-800-010) were purchased from the American Type Culture Collection (ATCC, Manassas, VA). Cells were suspended in IMDM containing 10% FBS (v/v; Hyclone), 1% HEPES (#15630080, ThermoFisher), and 1% penicillin-streptomycin (#15140122, ThermoFisher) and were immediately used.

METHOD DETAILS

Human Whole Blood Processing and Flow Cytometry
The study was approved by the Institutional Review Board of the University of Texas MD Anderson Cancer Center (#PA16-0971). The inclusion criteria of this study were as follows: 1) ≥ 18 years of age, 2) Karnofsky Performance Scale ≥ 70, 3) To receive radiation therapy (RT) with computed tomography (CT)-based treatment planning that will involve delivery of dose to the heart, 3) An estimated mean heart dose of at least 6 Gy and mean left ventricular dose of at least 5 Gy, as estimated by the treating radiation oncologist at the time of simulation.

The exclusion criteria of this study were as follows: 1) Unable or unwilling to give written informed consent, 2) Previous history of RT to the thorax or breast, 3) Allergy to gadolinium, 4) Implanted device that is non-MRI compatible, including cardiac devices and neurostimulators, 5) Pregnant or breast-feeding, 6) Atrial fibrillation or frequent ventricular or atrial premature beats, 7) GFR < 60 mL/min according to the Modification of Diet in Renal Disease equation, 8) Personal history of coronary artery disease or myocardial disease, 9) Personal history of hypertension, requiring >1 antihypertensive agent to maintain blood pressure <140/90, 10) Valvular stenosis or regurgitation of > moderate severity, 11) Heart failure (baseline NYHA >2), 12) Systolic BP <90 mmHg 15) Pulse <50/minute, 16) History of pulmonary hypertension or elevated right ventricular systolic pressures by echocardiogram, 17) Renal failure necessitating dialysis, 18) Suspicion or diagnosis of amyloidosis, 19) Suspicion or diagnosis of hemochromatosis, 20) Unable to obtain an MRI scan with gadolinium for any other reason that is not listed above.

Peripheral blood mononuclear cells (PBMCs) were isolated using a density technique with Histopaque-1077 from Sigma Aldrich. The blood was diluted with an equal amount of PBS (pH 7.4), 10 mL of which was layered over 10 mL of Histopaque-1077 and centrifuged at 400 xg for 35 minutes at ambient temperature in a swing-out rotor without the brake applied. PBMCs at the Histopaque-plasma interface was collected and washed twice with PBS by centrifugation at 300 xg for 10 minutes at 4°C. The cell number and viability were calculated using a hemocytometer. Non-viable cells were identified by staining with trypan blue, and cell viability was calculated using the total cell number count and non-viable cell count.

We measured p90RSK activity in circulating human $CD14^+$ cells as we described previously [7]. In brief, PBMCs were stainined with titrated volumes of antibodies against CD14-PE (8 μL), RSK-1-AF647 (5 μL), and phospho-p90RSK-AF488 (2 μL) for 30 minutes at 4 °C in the dark. Controls included cells that were incubated with or without the fluorochrome-conjugated antibodies. Fluorophore-positive gates were set with full-minus-one controls. Each sample was analyzed by sing an Accuri C6 flow cytometer (BD Biosciences, San Jose, CA) at a slow speed. FlowJo software (version 10.4.1, FlowJo LLC, Ashland, OR) was used to analyze the data. VersaComp antibody capture beads (#B22804, Beckman Coulter, Brea, CA) were used to calculate the compensation matrix.

Transfection

Cells were transfected with the appropriate plasmid DNAs using Lipofectamine 2000 transfection reagent according to the manufacturer's instructions. After transfection, cells were allowed to recover in the complete medium for 24 hours.

Western Blot Analysis

Macrophages were washed twice with cold PBS, and whole-cell lysates were prepared in RIPA buffer (50 mM Tris-HCl [pH 7.4], 150 mM NaCl, 1 mM EDTA, 1% Nonidet P40, 0.1% SDS, 1 mM dithiothreitol, 1:200-diluted protease inhibitor cocktail [P8340, Sigma-Aldrich], and 1 mM PMSF). Total lysates were resolved by SDS-PAGE and electrotransferred onto a Hybond-enhanced chemiluminescence nitrocellulose membrane, which was incubated with antibodies against each of the proteins to be detected in the lysate. Bound antibodies were visualized using the enhanced chemiluminescence detection reagents (Amersham Pharmacia Biotech, Little Chalfont, UK) according to the manufacturer's instructions and quantified by densitometry using ImageJ software. Tubulin was used as the loading control and was always probed together with the specific protein of interest. In most cases, anti-tubulin immunoblots are not shown to save space.

Efferocytosis Assay

BMDMs were cultured in IMDM containing 10% FBS (v/v; Hyclone), 1% HEPES, and 1% penicillin-streptomycin. To induce apoptosis in these cells, we treated 1 x 10^6 cells/mL in suspension with camptothecin (100 nM) for 6 hours and labeled them with IncuCyte pHrodo Red cell-labeling reagents (250 ng/mL) for 1 hour. For the efferocytosis assay, 1 x 10^4 BMDMs (effector cells) were plated on a 96-well flat-bottom plate; apoptotic cells were added to the surface of the adhered BMDMs.

After incubating the cells for 1 hour, we measured efferocytotic activity using IncuCyte ZOOM live cell imaging (ESSEN Bioscience, Ann Arbor, MI). Engulfment of pHrodo-labeled cells induces

pHrodo fluorescence by the phagosome's acidic environment, and the fluorescence intensity of the image was determined using IncuCyte ZOOM, as we previously reported [7].

ATP Assay
Intracellular ATP concentrations were measured using the ATP Assay Kit Colorimetric/Fluorometric (Abcam ab83355) per the manufacturer's protocol.

Measurement of NAD^+ Levels
NAD^+ was measured using the NAD^+/NADH quantification kit (Cell Biolabs, Inc., San Diego, CA) following the manufacturer's instructions. In brief, 5×10^5 cells seeded in 6-well plates were washed with cold PBS, collected, and centrifuged at 150 xg for 5 minutes. The cells were then resuspended in NAD extraction buffer, sonicated on ice and centrifuged at 14,000 xg for 5 minutes 4 °C to remove debris. The supernatant was filtered through a 10-kDa spin filter, and the flow through collected. The deproteinated cell extracts were transferred into a 96-well plate in duplicate, incubated with NAD Cycling Mix, and incubated for 2 hours at ambient temperature, protected from light. The plate was read with a fluorescence microplate reader that was equipped for excitation in the 530-570 nm range and for emission in the 590-600 nm range.

MTT [3-(4,5-Dimethylthiazol-2-yl)-2,5-Diphenyltetrazolium Bromide] Assay
Succinate dehydrogenase activity was evaluated using the Vybrant MTT cell proliferation kit (V13154, ThermoFisher) according to the protocols provided by the manufacturer. In brief, macrophages were seeded at a density of 5,000 cells/well in 96-well plates (#3882, ThermoFisher) and grown in IMDM with 10% FBS and 1% PS for 24 hours. Cells were then transferred to low serum (1% FBS) IMDM and treated with vehicle (PBS) or with the indicated doses of doxorubicin (DOX) for 24 hours or IR (24 hours after IR exposure). For the Vybrant MTT cell proliferation assay, cells were labeled with MTT at 1:10 dilution and incubated for 4 hours at 37 °C. Then, the 75 μL of medium was removed and 50 μL DMSO were added to each well and incubated cells for 10 minutes at 37 °C to solubilize the formazan crystals. Absorbance was measured at 540 nm was analyzed using a microplate reader (GenEX ThermoFisher).

Succinate dehydrogenase (SDH) activity assay
The SDH assay was performed with the SDH microplate assay kit (Abcam, #ab228560) by following the manufacturer's instructions.

Succinate assay
Succinate colorimetric assay kit (Abcam, #ab204718) was used to detect succinate level by following the manufacturer's instructions.

Secreted cytokines and chemokines assay
Mouse Inflammation array C1 kit AAM-INF-1 (Ray Biotech Inc., Norcross, GA) was used to detect various secreted cytokines and chemokines levels in the culture medium by following the manufacturer's instructions.

Lactate dehydrogenase (LDH) activity assay
Cell death induced by IR was measured by LDH activity into the cell culture medium. After 24 hrs IR treatment with the different doses, the culture medium was collected and centrifuged at 3,000 rpm for 5

min in order to take a cell-free supernatant. The LDH activity in the cell culture medium was measured with Cayman chemical kit (Item no 601170) by following the manufacturer's instructions.

Real-time PCR (RT-PCR)
At the end of experiments, BMDMs were washed 3 times with PBS and total cellular RNA isolated with TRIzol reagent (Invitrogen, #15596026). RTR-PCR wsa performed as we previously described[10]. Each reaction mixture (10 μ l) contained cDNA synthesized from 20 ng of total RNA, 5 μ l of iQ SYBR Green Supermix (1708882; Bio-Rad), and 0.5 μ mol/l each of forward and reverse primer, purchased from Origene with qSTAR quantitative PCR (qPCR) primers shown in Supplemental Table). Reactions were performed in triplicate. Real-time PCR was carried out using CFX96 Touch^{Tm} Real Time detection System (Bio-Rad) and SYBR Green (Bio-Rad) at thermal activation for 10 minutes at 95°C and 40 cycles of PCR (melting for 15 seconds at 95°C, followed by annealing/extension for 1 minute at 60°C). The $\Delta\Delta$Ct method was used to calculate fold changes in expression of target RNAs: ΔCt = Ct (target gene) – Ct (housekeeping gene, GAPDH); $\Delta\Delta$Ct = ΔCt (treatment) – ΔCt (control); and fold change = $2^{(-\Delta\Delta Ct)}$.

Metabolic Extracellular Flux Analysis (Seahorse)
The mitochondrial oxygen consumption rate (OCR) and extracellular acidification rate (ECAR) were assessed by using a Seahorse XF24 Extracellular Flux Analyzer (Agilent, Santa Clara, CA). BMDMs were pretreated with or without FMK-MEA (1 hour) in the presence or absence of IR or Dox. 25,000 cells of BMDMs per well were seeded into Seahorse XF24 cell culture microplates 16 hours before the assay and cultured with XF medium. Then, cells were cultured in Seahorse XF Base Medium supplemented with 1 mM pyruvate, 2 mM glutamine, and 10 mM D-glucose for the Seahorse XF cell mito stress test and with 1 mM glutamine for the Seahorse XF glycolysis stress test. The cell culture microplate was placed in a 37 °C non-CO_2 incubator for 1 hour and then loaded onto Seahorse XF24 to measure OCR and ECAR. The Seahorse XF mito stress test was performed sequentially under 4 conditions: 1) basal levels were measured with no additives; 2) oligomycin (1 μM), a reversible ATP synthase and OXPHOS inhibitor, was added to demonstrate glycolysis and mt leakage; 3) FCCP (1 μM), a mt uncoupler, was added to induce maximal OXPHOS; and 4) rotenone/antimycin A (0.5 μM), a complex I and III inhibitor, was added to end the mt reaction by shutting off mt respiration. The Seahorse XF glycolysis stress test was performed under 4 conditions: 1) basal level without glucose; 2) D-glucose (10 mM), which induces glycolysis; 3) oligomycin (1 μM), which inhibits OXPHOS and induces maximal glycolysis; and 4) 2-deoxy-glucose (2-DG, 50 mM), a glucose analog, which inhibits glycolysis through competitive binding to glucose hexokinase. After the Seahorse assay, the cells in the Seahorse XF cell culture microplate were stained with Hoescht 33342 and propidium iodide (ThermoFisher) to determine the numbers of total and dead cells, respectively. The live cell number should be the total Hoescht stained nuclei minus the propidium iodide-stained nuclei. All Seahorse measurements were normalized by the number of live cells in each well.

Telomere (TL) Length Assay
We measured TL length using the TL PNA kit/FITC (DAKO, Glostrup, Denmark) as we described previously [10]. In brief, BMDMs were suspended and washed by PBS and then incubated with the hybridization solution, supplemented with or without the fluorescein-conjugated PNA TL probe, and heated to 82 °C for 10 minutes. We performed hybridization in the dark at ambient temperature overnight. Cells were washed twice, for 10 minutes each at 40 °C, using the kit's washing solution. We

resuspended the cells in the DNA staining buffer and incubated for 1 hour at ambient temperature. After being washed, the cells were analyzed by a BD Accuri C6 Flow Cytometer using the FL-1 channel to detect the FITC signal and the FL-3 channel for propidium iodide. The human 1301 cell line (T-cell leukemia, #01151619-1VL, Sigma-Aldrich) was used as a control because these cells have unusually long TLs. We cultured 1301 cells in RPMI 1640 containing 2 mM L-glutamine and 10% FBS; the TL signal was measured as described above. The relative TL length was determined by calculating the ratio of the TL signal of each sample to the signal of 1301 cells after correcting for the DNA index of G0/1 cells for each cell type [7].

ERK5 Transcriptional Activity

We detected ERK5 transcriptional activity as we fully described previously [7]. Briefly, we transfected cells with Gal4-ERK5 and the Gal4-responsive luciferase reporter pG5-*luc* in Opti-MEM containing Lipofectamine 2000, per the manufacturer's instructions, for 16 hours. Cells were then treated by various cancer treatments (IR, Dox, ifosfamide, paclitaxel, or mitoxantrone), and luciferase activity was measured 36 hours after transfection using the dual luciferase kit (E1960, Promega, Madison, WI) by a TD-20/20 luminometer (Turner Designs, Sunnyvale, CA). Transfections were performed in triplicate, and each experiment was repeated at least 3 times [7].

High Throughput Screening

To establish a cell-based assay for ERK5 transcriptional activity, a HeLa cell line stably expressing pG5-Luc and pBIND-ERK5 vectors was generated as we reported previously[11]. In brief, we used the pG5-luc vector contains five Gal4 binding sites upstream of a minimal TATA box, which in turn, is upstream of the firefly luciferase gene, and the pBIND-ERK5 vector contains Gal4 fused with ERK5. Once ERK5 transcription activity is activated, Gal4 of pBIND-ERK5 binds with the Gal4 binding site of pG5-luc, and increased firefly luciferase expression. Cells were treated with compounds in the MicroSource SPECTRUM Collection for 18 hrs and luciferase activity determined.

NRF2-ARE Transcriptional Activity

We detected NRF2-ARE transcriptional activity as we fully described previously [7]. In brief, BMDMs were transfected using Opti-MEM, Lipofectamine 2000 with an ARE luciferase reporter and constitutively expressing *Renilla* luciferase vectors (ARE reporter kit, BPS Bioscience, San Diego, CA). After 16 hours of transfection, cells were treated with IR or DOX and collected after 36 hours of transfection to measure luciferase activity with a dual luciferase kit (E1960, Promega) and a TD-20/20 luminometer (Turner Designs). Transfections were performed in triplicate, and each experiment was repeated at least 3 times.

NF-κB Activity

BMDMs were transfected with the pNF-κB-Luc reporter plasmid, which contained 5 copies of the consensus NF-κB-responsive elements linked to a minimal E1B promoter-luciferase gene with pRL-TK (encoding Renilla luciferase). BMDMs were transfected with a mixture of the NF-κB-Luc and pRL-TK vectors using Lipofectamine 2000 in Opti-MEM according to the manufacturer's instructions. Cells were allowed to recover in normal IMDM for 30 hours and then treated with IR or Dox or vehicle control for 6 hours. The cells were harvested and assayed for firefly and Renilla luciferase activity using the Promega Dual-Luciferase Reporter Assay System.

Mitochondria-Specific Reactive Oxygen Species Measurements

We measured mitochondria-specific reactive oxygen species as we fully described previously [7]. Briefly, cells were incubated with MitoSOX Red (5 μM) (#M36008, Invitrogen, Eugene, OR), and fluorescence intensity was measured with excitation at 510 nm and emission at 580 nm using a plate reader (Biotek, Winooski, VT).

In Situ TUNEL Assay
TUNEL staining was performed using the ApopTag peroxidase *in situ* apoptosis detection kit (#S7100, Millipore) as we fully described previously [12].

Annexin V Apoptosis Assay
Annexin V apoptosis assay was performed using annexin V-fluorescein isothiocyanate (annexin V-FITC apoptosis detection kit, cat #ab14085, Abcam, Cambridge, MA) as we fully described previously [7].

Serum Lipid Profile Analysis
The levels of cholesterol (high- and low-density lipoprotein [HDL and LDL, respectively]) were determined using a cholesterol assay kit for mice (cat #EHDL-100, Bioassay System, Hayward, CA) as we fully described previously [7].

Housing and Husbandry
Mice were housed in pathogen-free conditions at The University of Texas MD Anderson Cancer Center as we fully described previously [13]. Briefly, the Program for Animal Resources is an AAALAC certified and defined pathogen-free facility for housing mice and rats, and a cage-level barrier system was used with an irradiated diet, ultra-filtered water, and heat-treated wood chip bedding.

Irradiation
Irradiation of the mouse's partial neck area was performed using the XRAD 225Cx (Precision X-ray Incorporated, North Branford, CT, USA). Mice were first placed in an inhalation anesthesia induction chamber and exposed to 5% isoflurane. After they had been fully anesthetized, they were placed on the radiation bed and maintained under anesthesia with 1.5%-2% isoflurane. To begin, we acquired a scout image of the mouse to target the partial neck and thoracic regions-of-interest for irradiation. After the target was set, radiation was delivered using a 30 x 30 mm collimator and copper filter in 2 fractions of 2.5 Gy, giving a total dose of 5 Gy. The anterior-posterior beam was delivered with 225 kVp for 50.72 seconds. The posterior-anterior beam was delivered with 225 kVp for 42.01 seconds.

The XRAD system is routinely checked using an ion chamber in air to ensure that the output of the system stays within 1% of desired output. The chamber has been calibrated by MD Anderson's Accredited Dosimetry Calibration Laboratory. The chamber calibration is traceable to the National Institute of Standards and Technology.

Echocardiography
Cardiac function was assessed before IR and TAC surgery and 4 weeks after surgery in sham- and TAC-operated mice, as we previously described [8]. We monitored anesthetized mice using a Vevo2100 echocardiography machine equipped with an MS-550D 40-MHz frequency probe (VisualSonics). LV (left ventricular) systolic and diastolic measurements were assessed in M-mode along the parasternal short axis of the LV. Fractional shortening was calculated using the following formula: %FS = (LV

end-diastolic diameter − LV end-systolic diameter)/(LV end-diastolic diameter) × 100. LV mass was calculated by 1.05 x [(IVSd (interventricular septal thickness diastole) + LVIDd (LV internal dimensions diastole) + PWd (posterior wall thickness)3-LVIDd3), as previously described [14].

Monitoring of Mice after Surgery

After TAC surgery, mice were monitored in a chamber on a heating pad and pre-warmed normal saline (37 °C, 5 ml per 100 g body weight) was given subcutaneously. Post-operative mice were monitored as we described fully in our previous report [7] and also described in our Institutional Animal Use and Care Committee-approved protocol.

Histological Evaluation (Mouse Coronary Artery) and Immunostaining (Heart)

Mouse hearts were harvested and fixed for 24 hours in 10% formalin and embedded in paraffin after the dehydration procedure by using an automated tissue processor (LEICA, TP1020). We evaluated coronary artery lesions using the method described by Marino et al. with a small modifications [15]. The whole heart was sectioned systematically from the aortic valve area (level 0) all the way to the apex (level 11). We made 8 serial sections (5 µm thick) at each of the 12 levels that were equally spaced by a 400 µm interval. One slide from every level was used for H&E staining for studying the cardiac and left anterior descending artery (LAD) histology. To assess the vascular wall thickness of LAD , we first determined the short axis of cross-sectioned LAD in each section and drew a line representing the axis over the vessel. The vessel diameter was defined as the distance between the two outer edges of the media along this short axis line. Next, we measured the wall thickness (the intima plus media thickness) along the line, which yielded two measurements. These two values were averaged, and this value was divided by the vessel diameter. This process was repeated at all levels of a given heart. We found that the wall-thickness/vessel-diameter ratios calculated for different levels of a heart were surprisingly similar. We took the average of these ratios and defined it as the LAD wall thickness index of a given heart. These values were compared among various animals with different treatments. Vessels with atherosclerotic lesion were excluded from this analysis. Stenosis by atherosclerotic plaques was evaluated by a modified stenosis grading system; grade 0 (0% of the luminal area), grade 1 (<33%), grade 2 (33-66%), and grade 3 (66%<), as reported previously [16].

For the immunofluorescence analysis, the heart sections were incubated for 1 hour at 60 °C, deparaffinized in fresh xylene, and rehydrated through a graded alcohol series. After a PBS wash, antigen retrieval was performed for 12 minutes at 95 °C in 10 mM sodium citrate buffer (pH 6.0) containing 0.05% Tween 20. Slides were washed with PBS and treated with Dako Protein Block Serum-free (#S3020, Dako) containing 10% normal donkey serum for 1 hour at ambient temperature to block non-specific antibody binding. The slides were incubated overnight at 4 °C with anti-CD31 (1:15, #AF3628, R&D Systems; Minneapolis, MN) and anti-MAC3 (1:150, #550292, BD Biosciences; San Jose, CA). After being washed with PBS-T (PBS containing 0.2% Tween 20) and PBS, the slides were incubated with Alexa488 anti-Goat secondary antibody (1:2000, #A11055, Invitrogen), Alexa546 anti-Rat secondary antibody (1:2000, #A11081, Invitrogen), and DAPI (2.5 ug/mL, #D1306, Invitrogen) for 1 hour at ambient temperature. After being washed with PBS-T (PBS containing 0.2% Tween 20) and PBS, the slides were mounted using ProLong Gold Antifade Mountant (#P36930, Invitrogen) Immunofluorescence images were captured by Olympus FX1200 MPE confocal laser scanning microscope. We picked 2 slides, each from different levels (around section level 5 (#5) and level 10 (#10)), and performed anti-CD31/anti-MAC3 double immunofluorescence staining. To define the perivascular area, we first defined the vessel redius as the distance from the center of the vessel to

the outer edge of the media (along the short axis of the vessel defined earlier) and then defined the perivascular region as the area between the outer edge of media and one radius distance away from it. This area is shown as that between two dotted lines in the figure. We counted the number of MAC3-positive cells within this area, divided it by this areain each slide, and averaged the numbers from 2 sections for each heart.

Sirius Red staining was performed with the Picro Sirius Red Stain Kit (#ab150681, Abcam) according to the manufacturer's instruction. We picked 2 slides from different levels (around section #5 and #10) from each heart and assessed the LAD fibrosis and the interstitial fibrosis. For the LAD fibrosis, the Sirius Red-posivtivearea in the media and perivascular region was measured by ImageJ software and normalized by the luminal area. For the interstitial fibrosis, Sirius Red-stained sections were captured by the Vectra Polaris Imaging System (Akoya Biosciences; Menlo Park, CA), and the red-stained area was normalized by the total tissue area (%). We averaged data from the 2 slides in each sample.

Masson's trichrome staining was performed with the Trichrome Stain Kit (#ab150686, Abcam) according to the manufacturer's instructions.

Detecting *in Vivo* Priming of CD11b-Positive Cells in Mice Exposed to IR

C57BL/6 mice were IP injected with olaparib (10 mg/kg body weight) once a day 1 day before and after IR and on the day of IR. After 72 hours of whole-body radiation (2 Gy), we isolated PBMCs from whole blood by density gradient centrifugation using Histopaque 1077 (Sigma-Aldrich, cat#10771) following the manufacturer's instructions. p90RSK activation was detected as stated in the section of "Human Whole Blood Processing and Flow Cytometry".

STATISTICAL ANALYSIS

For the *in vitro* and *in vivo* statistical analyses, we determined differences between 2 independent groups using the Student *t*-test (2-tailed) and, when applicable, 1-way analysis of variance, followed by Bonferroni post hoc testing for multiple group comparisons using GraphPad Prism (GraphPad Software, San Diego, CA, USA) (except Figure 8D). In Figure 8D, we used repeated measures 1-way ANOVA, with the Geisser-Greenhouse correction, followed by Turkey's multiple comparison test, with individual variances computed for each comparison. When groups exhibited unequal variances, we used Welch's analysis of variance to perform multiple group comparisons. *P* values <0.05 were considered statistically significant, and are indicated by 1 asterisk in the figures. *P* values <0.01 are indicated by 2 asterisks. All continuous variables were assumed to be normally distributed. Since a large number of statistical comparisons was performed, all at the 0.05 significance level, there was the possibility of a type I error.

SUPPLEMENTARY TABLE: Lisat of qRT-PCR primers

Primers	Sequences
IL-1b -F	5′-CTACAGGCTCCGAGATGAACAA-3′
IL-1b-R	5′-TCCATTGAGGTGGAGAGCTTTC-3′
TNFa-F	5′-GGCTGCCCCGACTACGT-3′
TNFa-R-	5′-AGGTTGACTTTCTCCTGGTATGA-3′
b-ACTIN-F	5′-AGAGGGAAATCGTGCGTGAC-3′
b-ACTIN-R	5′-CAATAGTGATGACCTGGCCGT-3′
iNOS-F	5′-TCCTGGAGGAAGTGGGCCGAAG3′-
iNOS-R	5′-CCTCCACGGGCCCGGTACTC-3′
Arg1-F	5′-CAGAAGA- ATGGAAGAGTCAG-3′
Arg1-R	5′-CAGATATGCAGGGAGTCAC- C-3′
Ym1-F	5′-GCAGAAGCTCTCCAGAAGCAATCCTG-3
Ym1- R	5′-ATTGGCCTGTCCTTAGCCCAACTG-3′
Fizz1-F	5′-GCTGATGGTCCCAGTGAATAC-3
Fizz1-R	5′-CCAGTAGCAGTC- ATCCCAGC-3′

SUPPLEMENTARY FIGURE LEGENDS

Supplementary Figure 1. Time courses and dose response of proteins shown in Figure 1A; IR increased p90RSK activity, which phosphorylated ERK5 S496, but not the TEY motif, in a time-dependent manner, and Dox induced SASP via p90RSK activation. (A, B) The graphs represent densitometry data from 3 independent gels, one of which is shown in Figure 1A. The data are mean±SD, $^{**}P<0.01$. **(C)** Human monocytes were pre-treated with a p90RSK-specific inhibitor of FMK-MEA (10 μM) or vehicle (DMSO, 0.1%) for 1 hour and then treated with DOX (1 μM) for the time indicated (0-60 minutes). Western blot analyses were performed using the indicated antibodies. **(D)** Quantification of the DOX-induced p90RSK activation (S380 phosphorylation; left), ERK5 S496 phosphorylation (middle), and ERK5 activation (TEY motif phosphorylation; right) is shown after normalization by each total protein level. The data represent the mean±SD (n=3). $^{**}P<0.01$ and $^{*}P<0.05$. **(E)** BMDMs were pre-treated with FMK-MEA (10 μM) or vehicle for 1 hour, and cells were treated with Dox (1 μM) for 0-24 hours. Western blot analyses were performed using specific antibodies against the proteins indicated on the right. Representative images from 3 independent experiments are shown. **(F)** The graphs represent densitometry data from 3 independent gels, one of which is shown in **E**. The data are mean±SD, n=3, $^{**}P<0.01$.

Supplementary Figure 2. Secreted cytokines and chemokines induced by low dose of IR and DOX-induced M1-like phenotype are p90RSK activity dependent. (A) BMDMs from WT mice were pre-treated with FMK-MEA (10 μM) or vehicle for 1 hour and then exposed to IR, and after 24 hrs of IR, the indicated cytokines and chemokines secreted in the cell culture medium were measured by mouse inflammation array C1 AAM-INF-1 kit (Ray Biotech Inc., Norcross, GA). **(B, C)** BMDMs from WT mice were pre-treated with FMK-MEA (10 μM) or vehicle for 1 hour and then exposed to IR, and after 24 hrs of IR, the expressions of M1- **(B)** and M2 **(C)** -like markers mRNA levels were detected by the fold inductions relative to the expression in unexposed BMDMs. The data are mean±SD, n=3, $^{**}P<0.01$, $^{*}P<0.05$.

Supplementary Figure 3. Various cancer treatments increased p90RSK activity, which then phosphorylated ERK5 S496, but not the TEY motif, in a time- and dose-dependent manner and inhibited ERK5 transcriptional activity via p90RSK activation (DOX and ifosfamide). BMDMs from C57Bl/6 mice were treated with various types of cancer treatments for various lengths of time (**A, B, F, G**): **A,B**: DOX (1 μM), **F, G**: ifosfamide (10 μM), and various concentrations of cancer treatments for 10 minutes (**C, D, H, and I**). Western blot analyses were performed using specific antibodies against the proteins indicated on the right side of gels. The graph represents densitometry data from 3 independent experiments. **(E, and J)** BMDMs were transfected with pBind vector containing ERK5, pG5-luc plasmids, and pcDNA3.1 plasmid (as a control) or CA-MEK5 for 30 hours; they were then pre-treated with p90RSK-specific inhibitor, FMK-MEA (10 μM), or vehicle for 1 hour, followed by incubation with Dox (1 μM) **(E)**, ifosfamide (10 μM) **(I)**, or vehicle (DMSO, 0.1%) for 6 hours. ERK5 transcriptional activity was measured as described in the Methods. Mean±SD, $^{**}P<0.01$, and $^{*}P<0.05$.

Supplementary Figure 4. Various cancer treatments increased p90RSK activity, which then phosphorylated ERK5 S496, but not the TEY motif, in a time- and dose-dependent manner and inhibited ERK5 transcriptional activity via p90RSK activation (paclitaxel and methotrexate). BMDMs from C57Bl/6 mice were treated with various types of cancer treatments for various lengths of

time (**A, B, F, and G**): **A, B**: paclitaxel (2 μM). **F, G**: methotrexate (MTX, 5 μM), and various concentrations of cancer treatments for 10 minutes (**C, D, H** and **I**). Western blot analyses were performed using specific antibodies against the proteins indicated on the right side of gels. The graph represents densitometry data from 3 independent experiments. **(E,** and **J)** BMDMs were transfected with pBind vector containing ERK5, pG5-luc plasmids, and pcDNA3.1 plasmid (as a control) or CA-MEK5 for 30 hours; they were then pre-treated with p90RSK-specific inhibitor, FMK-MEA (10 μM), or vehicle for 1 hour, followed by incubation with paclitaxel (2 μM) **(E)**, MTX (5 μM) **(I)**, or vehicle (DMSO, 0.1%) for 6 hours. ERK5 transcriptional activity was measured as described in the Methods. Mean±SD, $^{**}P<0.01$, and $^{*}P<0.05$.

Supplementary Figure 5. IR- and Dox-induced SASP events were inhibited by p90RSK-specific inhibitors (FMK-MEA and BI-D1870) and DN-p90RSK, and IR- and Dox-induced TL shortening by inhibiting NRF2 transcriptional activity. (A, B) IR and p90RSK-specific inhibitors: BMDMs were transfected with the ARE luciferase reporter and the constitutively expressing *Renilla* luciferase vector for 16 hours. Cells were pre-treated with FMK-MEA (10 μM) **(A)** or BI-D1870 (10 μM) **(B)** for 1 hour and then exposed to IR or non-IR. After 6 hours of IR, NRF2-ARE transcriptional activity was measured as described in Methods. **(C-F)** IR and DN-p90RSK: BMDMs isolated from WT and DN-RSK-MTg mice were transfected with the ARE luciferase reporter and the constitutively expressing *Renilla* luciferase vector for 16 hours **(C)** and then exposed to IR or non-IR. After 6 hours of IR, NRF2-ARE transcriptional activity was measured as described in Methods. **(D)** BMDMs isolated from WT and DN-*p90rsk*-MTg mice were treated with IR (2 Gy). After 24 hours of IR, TL lengths were determined by measuring the fluorescent telomeric signal intensity of the fluorescein-conjugated PNA probe, as described in Methods. **(E)** BMDMs from WT and DN-*p90rsk*-MTg mice were transfected with the NF-κB luciferase reporter and the constitutively expressing *Renilla* luciferase vector for 16 hours. After 12 hours of IR, NF-κB transcriptional activity was measured as described in Methods. **(F)** BMDMs isolated from WT and DN-*p90rsk*-MTg mice were treated with IR (2 Gy); after 24 hours of IR, cells were incubated with the IncuCyte pHrodo-labeled apoptosis detection probe, and pHrodo-positive cells were quantified. **(G-I)** Dox and p90RSK inhibitors and DN-p90RSK: BMDMs were transfected with ARE luciferase reporter and the constitutively expressing *Renilla* luciferase vector for 16 hours, pre-treated with FMK-MEA (left) or BI-D1870 (right) for 1 hour, and treated with Dox (1 μM) or vehicle for 18 hours. NRF2-ARE transcriptional activity was measured as described in Methods. **(H)** BMDMs were pre-treated with FMK-MEA for 1 hour and Dox (1 μM) for 24 hours. TL lengths were determined as described in Methods. **(I)** BMDMs were transfected with the NF-κB luciferase reporter and the constitutively expressing *Renilla* luciferase vector for 16 hours. Cells were pre-treated with FMK-MEA or BI-D1870 for 1 hour and then incubated with Dox or vehicle for 12 hours; NF-κB transcriptional activity was measured as described in Methods. The data are mean±SD, n=3, $^{**}P<0.01$. **(J)** BMDMs were transfected with the ARE luciferase reporter and the constitutively expressing *Renilla* luciferase vector for 16 hours. Cells were pre-treated with NRF2A (CAS 1362661) or vehicle for 6 hours and IR (2 Gy) or Dox (1 μM); After 18 hours of the treatments NRF2-ARE transcriptional activity from 3 independent experiments was measured as described in Methods. **(K)** BMDMs were pre-treated with NRF2A for 1 hour and then treated with IR (2 Gy) or Dox (1 μM). After 24 hours of the treatments TL lengths were determined as described in Methods. The data are mean±SD, n=3, $^{**}P<0.01$.

Supplementary Figure 6. Dox (1 μM) remarkably inhibited both OXPHOS and glycolysis by p90RSK activation, IR- and Dox-induced PARP activation via p90RSK-ERK5 S496 phosphorylation (quantification), and IR and Dox upregulated p90RSK-ERK5 S496 phosphorylation via mtROS. BMDMs were seeded in Seahorse plates. BMDMs isolated from WT were pre-treated with FMK-MEA (10 μM) or vehicle for 1 hour and then treated with Dox (1 μM) **(A-D)**. After 24 hours, OXPHOS and glycolysis parameters were detected. During extracellular flux analysis, cells were sequentially treated with **(A)** OM, FCCP, and rotenone (ROT) plus antimycin A (AA) to assess OXPHOS parameters from the OCR levels. **(B)** The basal respiration, mitochondrial ATP production, maximal respiration, and spare respiratory capacity were calculated and plotted as OCR in pmoles/minutes/50,000 cells (n=3, mean±SD, $^{**}P<0.01$) or with **(C)** glucose, OM, and 2-deoxyglucose (2-DG), to determine glycolysis parameters from the ECAR levels. **(D)** Glycolysis, glycolytic reserve, glycolytic capacity, and non-glycolytic acidification were calculated and plotted as ECAR in mpH/minutes/50,000 cells. n=3, mean±SD, $^{**}P<0.01$. **(E-G)** The graphs represent densitometry data from 3 independent gels, one of which is shown in Figure 6A (**E**) and Figure 6B (**F**). The data are mean±SD, n=3, $^{**}P<0.01$. (**G**) BMDMs were pre-treated with olaparib (10 μM) or vehicle for 1 hour and then incubated with DOX (1 μM) for 16 hours. MitoSox Red was added, and mt ROS levels were detected as described in Methods. Mean±SD, n=3, $^{**}P<0.01$. **(H-I)** BMDMs were treated with MitoTEMPOL (10 μM) for 1 hour and treated with IR **(H)** or DOX **(I)**, as indicated, for 0-60 minutes (for IR, times indicated are post-IR incubation time). Western blot analyses were performed using specific antibodies against the indicated proteins. The graphs represent densitometry data from 3 independent gels. The data are mean±SD, n=3, $^{**}P<0.01$.

Supplementary Figure 7. Transient PARP inhibition and IR (localized 5 Gy twice)-induced cardiac interstitial and perivascular fibrosis after TAC, and body weights and serum cholesterol levels in olaparib-treated *Ldlr*$^{-/-}$ mice after TAC with HFD. (A) Representative H&E staining and immunofluorescence staining of a coronary artery with atherosclerosis for CD31 (endothelial cells [green]), Mac3 (macrophages [red]), and DAPI (nucleus [blue]). **(B)** Representative Sirius staining of the whole heart. The Sirius stained area within each of the whole heart sections (shown on the left) was determined using ImageJ software. Mean±SD. **(C)** Representative Sirius staining of a perivascular region. The area of Sirius staining in media and perivascular area was determined using ImageJ software. Mean±SD. $^{*}P<0.05$. **(D, E)** Body weight **(D)** and HDL and LDL levels **(E)** in olaparib- or vehicle-treated *Ldlr*$^{-/-}$ mice after TAC or IR.

Supplementary Figure 8. IR-induced MC reprogramming, priming, and coronary disease. The details were discribed in the discussion. Created with Biorender.com

REFERENCES

1.Krischke M, Hempel G, Voller S, Andre N, D'Incalci M, Bisogno G, Kopcke W, Borowski M, Herold R, Boddy AV, Boos J. Pharmacokinetic and pharmacodynamic study of doxorubicin in children with cancer: results of a "European Pediatric Oncology Off-patents Medicines Consortium" trial. Cancer Chemother Pharmacol 2016;**78**(6):1175-1184.
2.Kurowski V, Wagner T. Comparative pharmacokinetics of ifosfamide, 4-hydroxyifosfamide, chloroacetaldehyde, and 2- and 3-dechloroethylifosfamide in patients on fractionated intravenous ifosfamide therapy. Cancer Chemother Pharmacol 1993;**33**(1):36-42.
3.Nannan Panday VR, de Wit R, Schornagel JH, Schot M, Rosing H, Lieverst J, ten Bokkel Huinink WW, Schellens JH, Beijnen JH. Pharmacokinetics of paclitaxel administered in combination with cisplatin, etoposide and bleomycin in patients with advanced solid tumours. Cancer Chemother Pharmacol 1999;**44**(4):349-53.
4.Balis FM, Holcenberg JS, Poplack DG, Ge J, Sather HN, Murphy RF, Ames MM, Waskerwitz MJ, Tubergen DG, Zimm S, Gilchrist GS, Bleyer WA. Pharmacokinetics and pharmacodynamics of oral methotrexate and mercaptopurine in children with lower risk acute lymphoblastic leukemia: a joint children's cancer group and pediatric oncology branch study. Blood 1998;**92**(10):3569-77.
5.McBeath E, Parker-Thornburg J, Fujii Y, Aryal N, Smith C, Hofmann MC, Abe JI, Fujiwara K. Rapid Evaluation of CRISPR Guides and Donors for Engineering Mice. Genes (Basel) 2020;**11**(6).
6.Norton WB, Scavizzi F, Smith CN, Dong W, Raspa M, Parker-Thornburg JV. Refinements for embryo implantation surgery in the mouse: comparison of injectable and inhalant anesthesias - tribromoethanol, ketamine and isoflurane - on pregnancy and pup survival. Lab Anim 2016;**50**(5):335-43.
7.Singh MV, Kotla S, Le NT, Ae Ko K, Heo KS, Wang Y, Fujii Y, Thi Vu H, McBeath E, Thomas TN, Jin Gi Y, Tao Y, Medina JL, Taunton J, Carson N, Dogra V, Doyley MM, Tyrell A, Lu W, Qiu X, Stirpe NE, Gates KJ, Hurley C, Fujiwara K, Maggirwar SB, Schifitto G, Abe JI. Senescent Phenotype Induced by p90RSK-NRF2 Signaling Sensitizes Monocytes and Macrophages to Oxidative Stress in HIV-Positive Individuals. Circulation 2019;**139**(9):1199-1216.
8.Knight WE, Chen S, Zhang Y, Oikawa M, Wu M, Zhou Q, Miller CL, Cai Y, Mickelsen DM, Moravec C, Small EM, Abe J, Yan C. PDE1C deficiency antagonizes pathological cardiac remodeling and dysfunction. Proc Natl Acad Sci U S A 2016;**113**(45):E7116-E7125.
9.Englen MD, Valdez YE, Lehnert NM, Lehnert BE. Granulocyte/macrophage colony-stimulating factor is expressed and secreted in cultures of murine L929 cells. J Immunol Methods 1995;**184**(2):281-3.
10.Kotla S, Vu HT, Ko KA, Wang Y, Imanishi M, Heo KS, Fujii Y, Thomas TN, Gi YJ, Mazhar H, Paez-Mayorga J, Shin JH, Tao Y, Giancursio CJ, Medina JL, Taunton J, Lusis AJ, Cooke JP, Fujiwara K, Le NT, Abe JI. Endothelial senescence is induced by phosphorylation and nuclear export of telomeric repeat binding factor 2-interacting protein. JCI Insight 2019;**4**(9).
11.Le NT, Takei Y, Izawa-Ishizawa Y, Heo KS, Lee H, Smrcka AV, Miller BL, Ko KA, Ture S, Morrell C, Fujiwara K, Akaike M, Abe J. Identification of activators of ERK5 transcriptional activity by high-throughput screening and the role of endothelial ERK5 in vasoprotective effects induced by statins and antimalarial agents. J Immunol 2014;**193**(7):3803-15.
12.Heo KS, Cushman HJ, Akaike M, Woo CH, Wang X, Qiu X, Fujiwara K, Abe J. ERK5 activation in macrophages promotes efferocytosis and inhibits atherosclerosis. Circulation 2014;**130**(2):180-91.
13.Ko KA, Wang Y, Kotla S, Fujii Y, Vu HT, Venkatesulu BP, Thomas TN, Medina JL, Gi YJ, Hada M, Grande-Allen J, Patel ZS, Milgrom SA, Krishnan S, Fujiwara K, Abe JI. Developing a Reliable

Mouse Model for Cancer Therapy-Induced Cardiovascular Toxicity in Cancer Patients and Survivors. Front Cardiovasc Med 2018;**5**:26.
14.Gao S, Ho D, Vatner DE, Vatner SF. Echocardiography in Mice. Curr Protoc Mouse Biol 2011;**1**:71-83.
15.Marino A, Zhang Y, Rubinelli L, Riemma MA, Ip JE, Di Lorenzo A. Pressure overload leads to coronary plaque formation, progression, and myocardial events in ApoE-/- mice. JCI Insight 2019;**4**(9).
16.Kosuge H, Haraguchi G, Koga N, Maejima Y, Suzuki J, Isobe M. Pioglitazone prevents acute and chronic cardiac allograft rejection. Circulation 2006;**113**(22):2613-22.

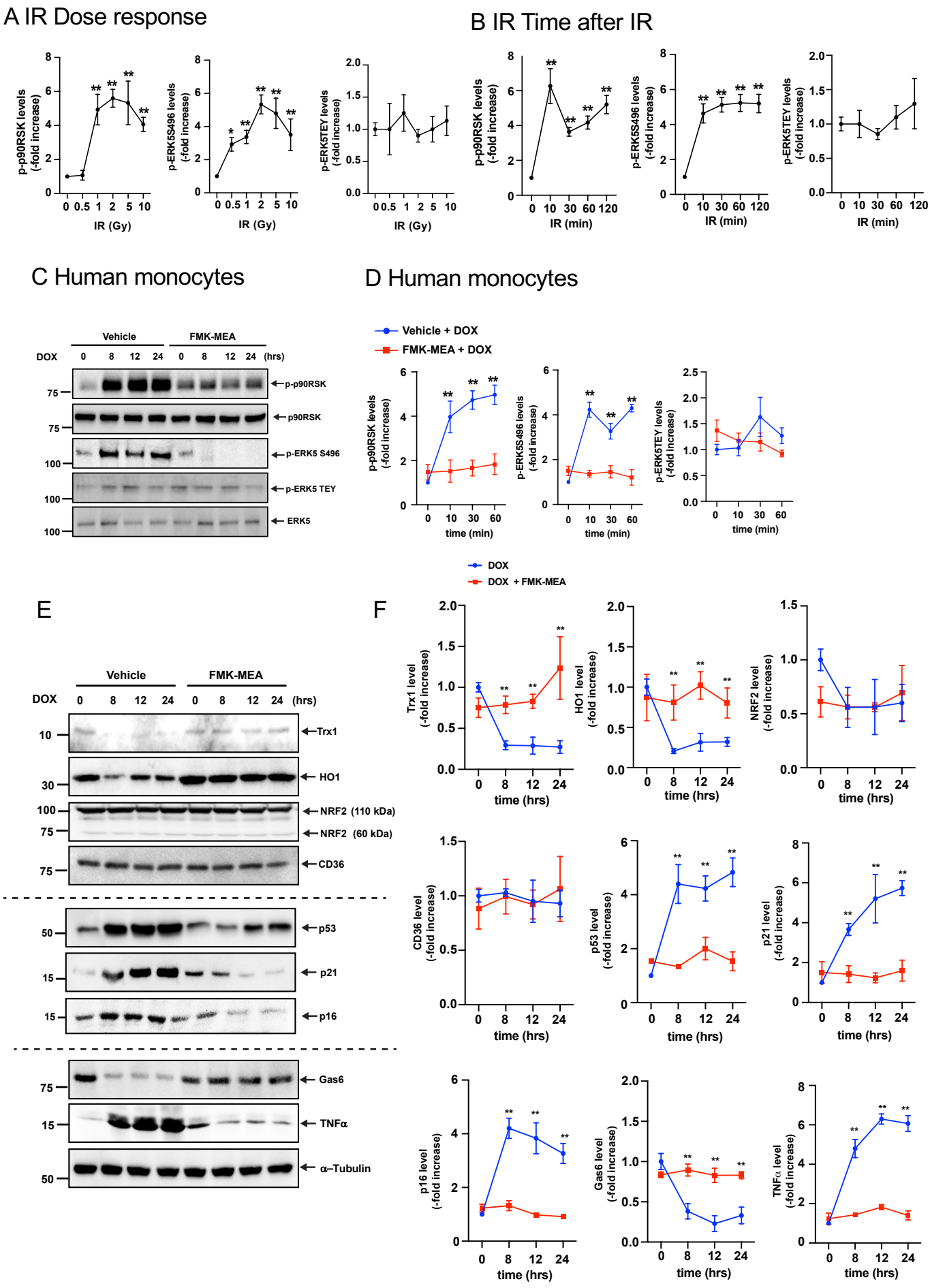

Supplementary Figure 1

A. Secretion of various cytokines and chemokines

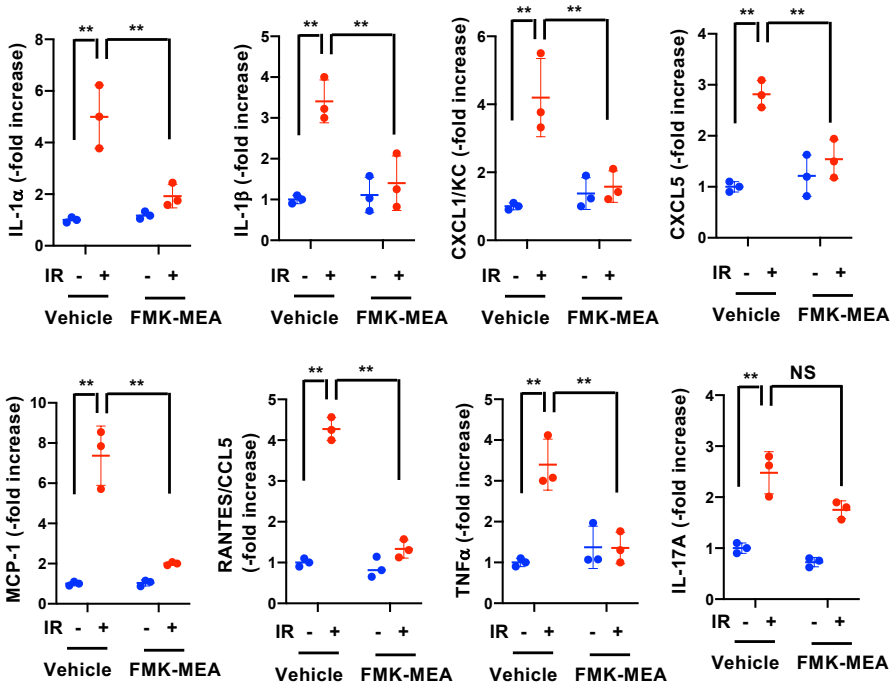

B

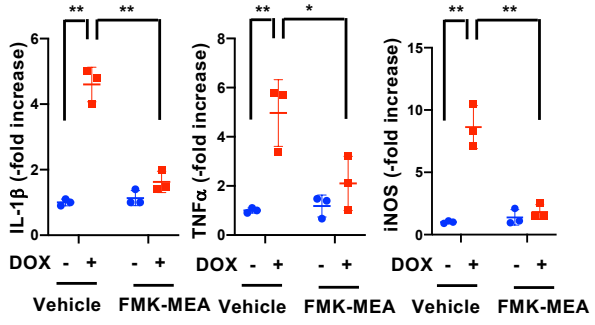

C

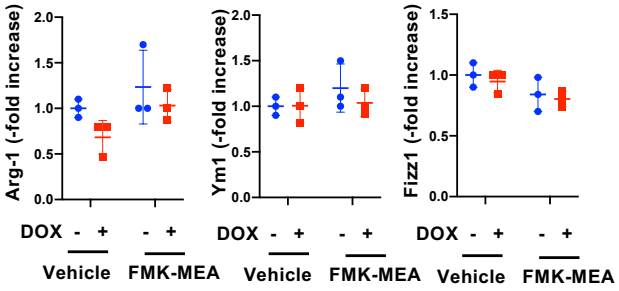

Supplementary Figure 2

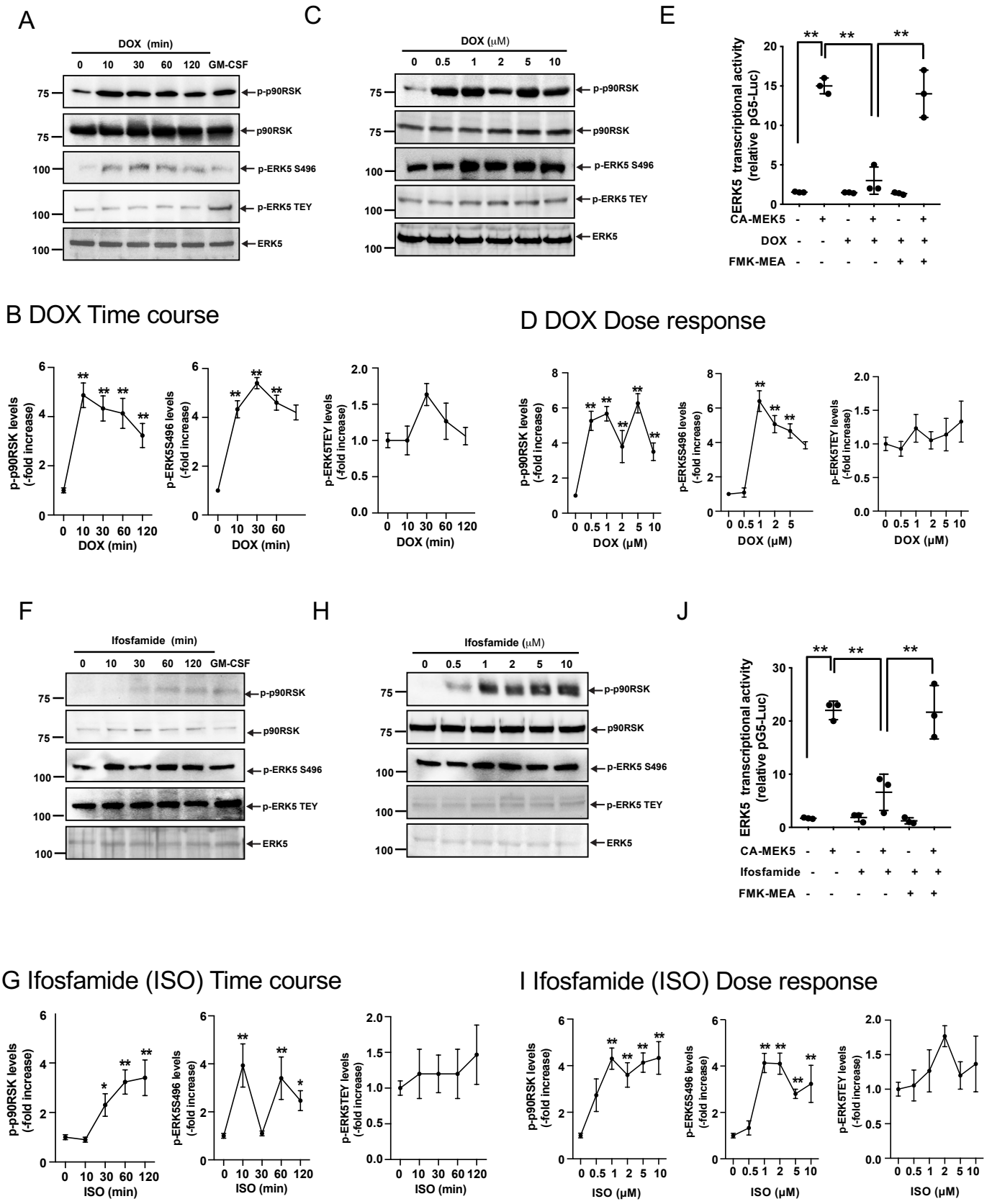

Supplementary Figure 3

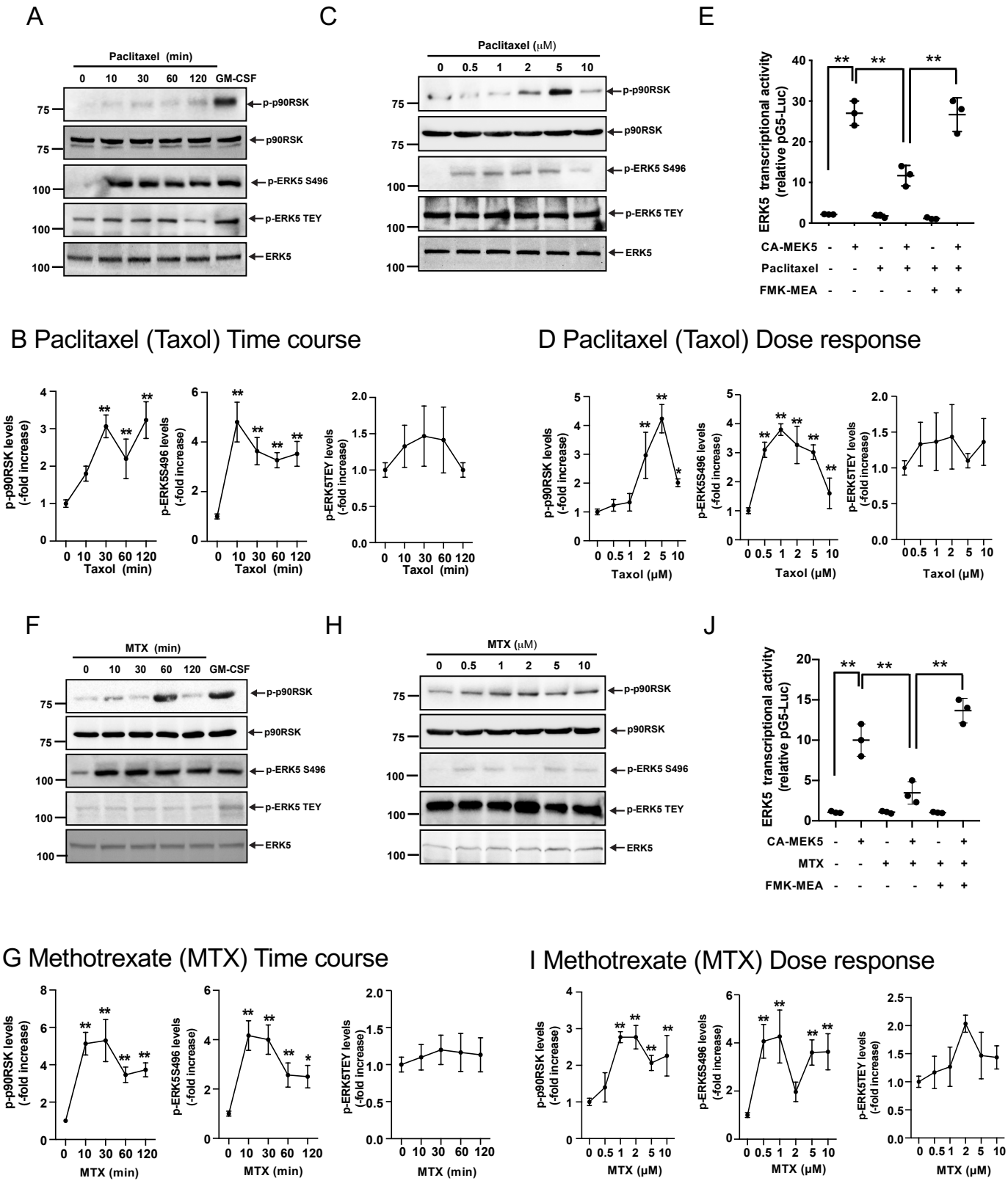

Supplementary Figure 4

IR and p90RSK inhibitors

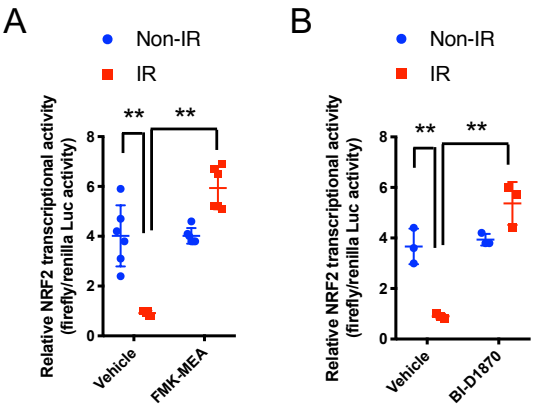

IR and DN-RSK

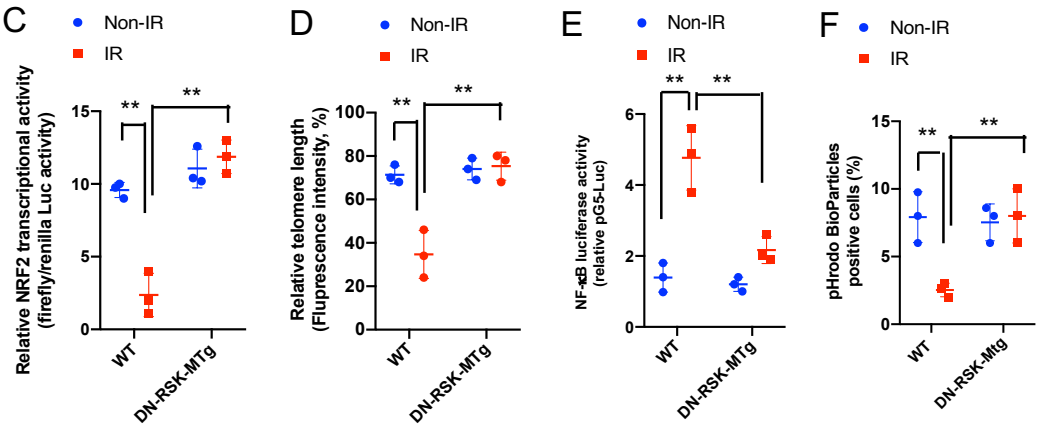

DOX and p90RSK inhibitors and DN-RSK

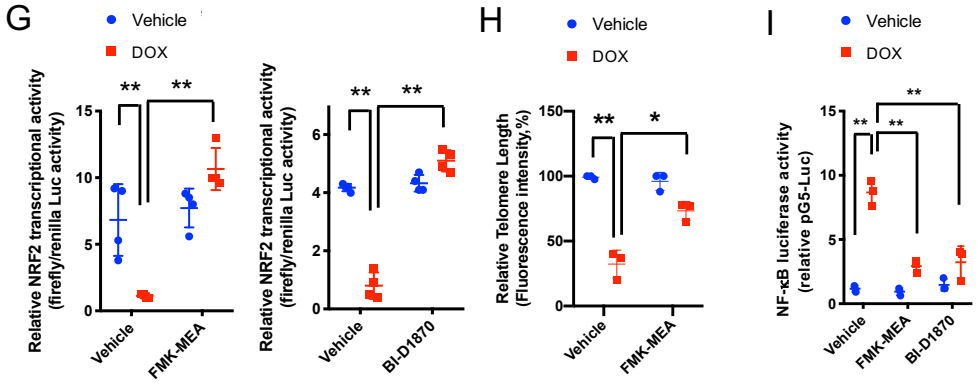

J NRF2A

K NRF2A

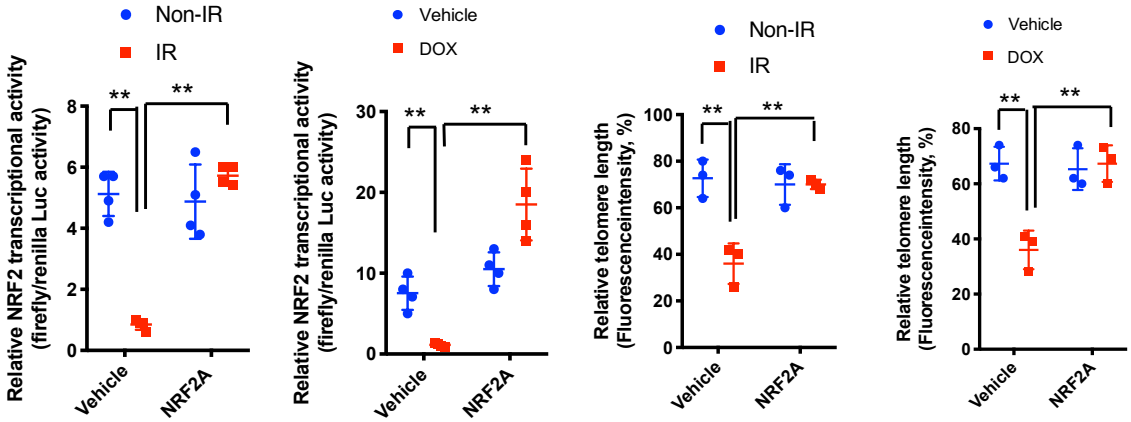

Supplementary Figure 5

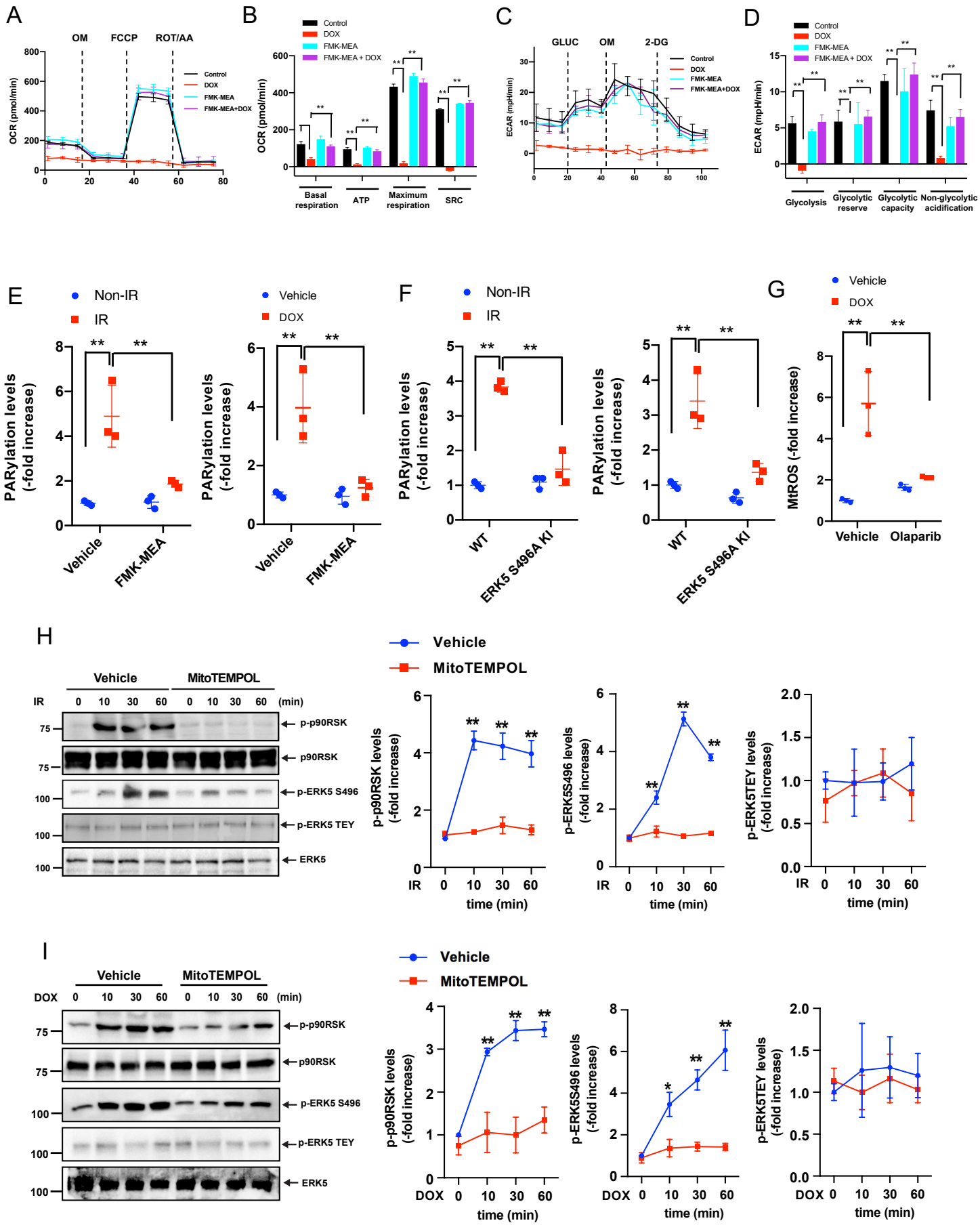

Supplementary Figure 6

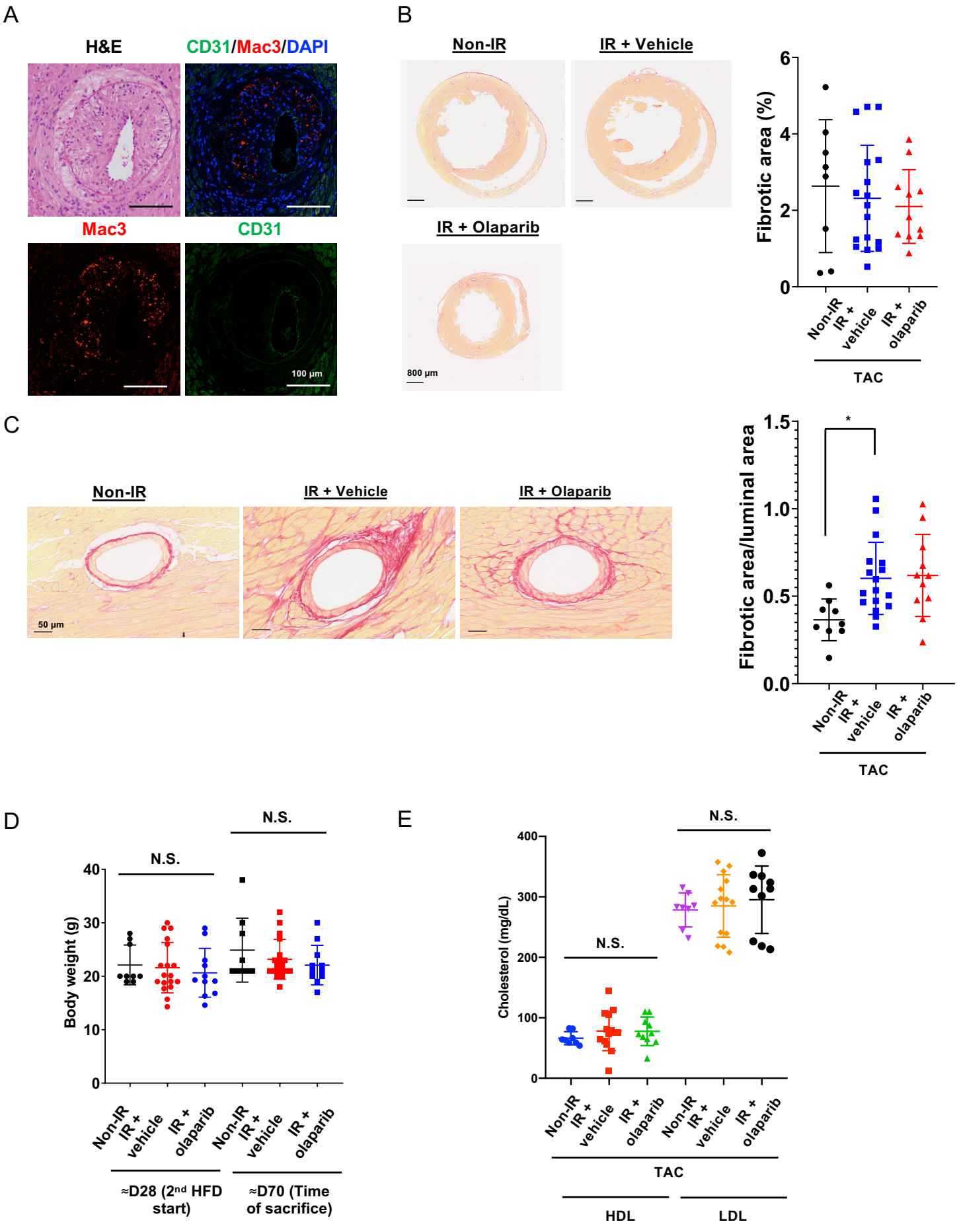

Supplementary Figure 7

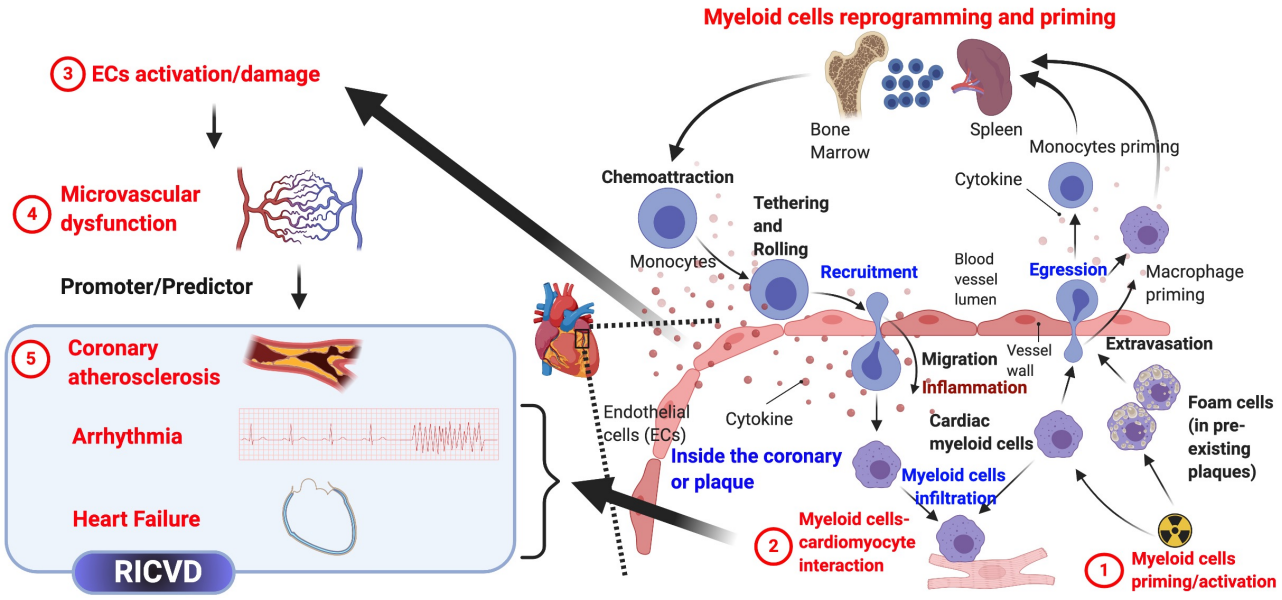

Supplementary Figure 8

Figure 1A (Un-cropped)

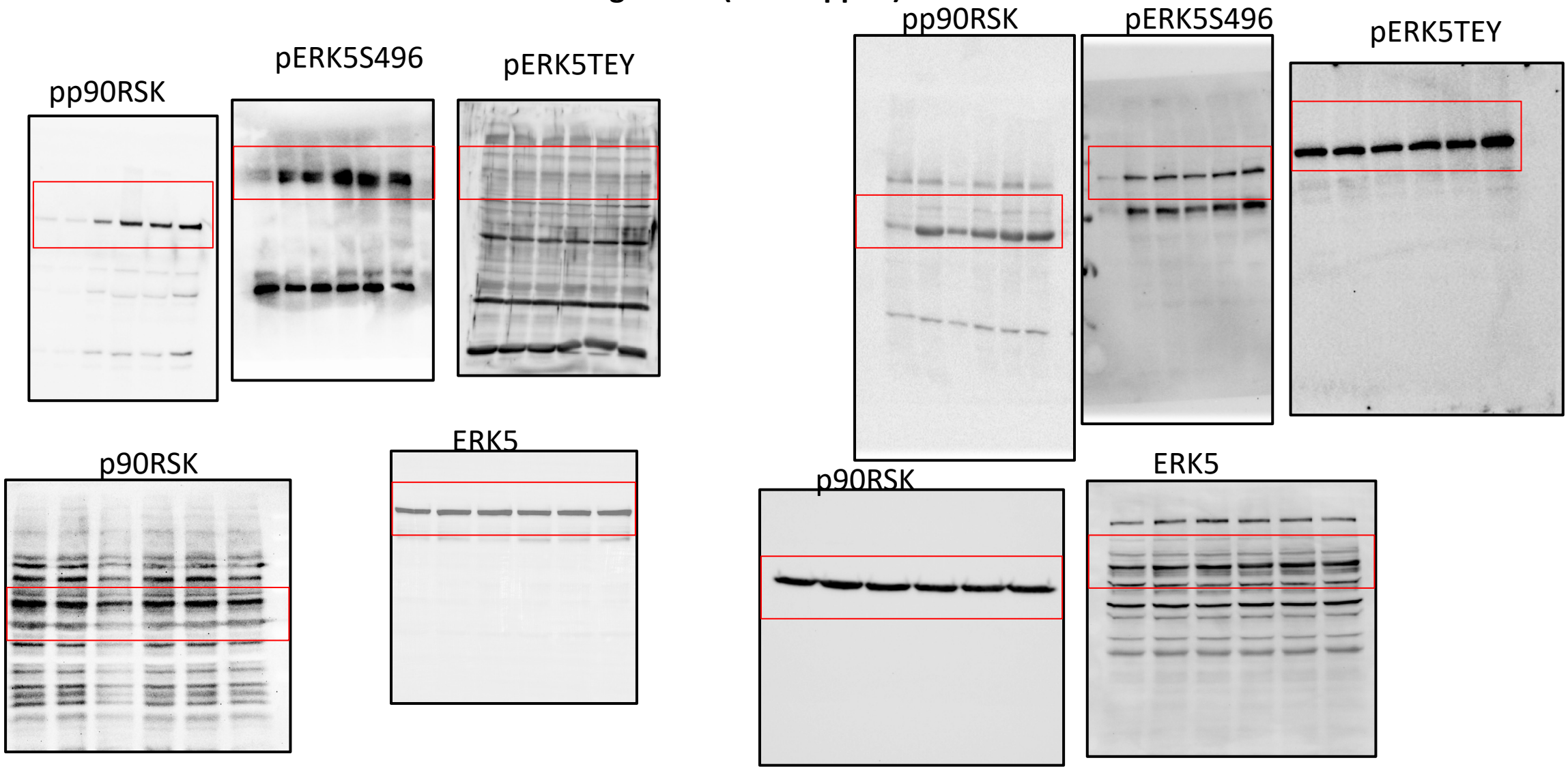

Figure 1D (Un-cropped)

pp90RSK

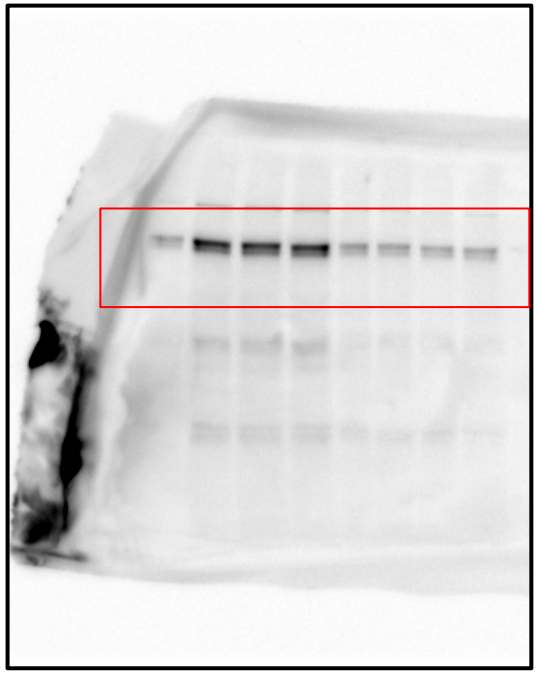

p90RSK

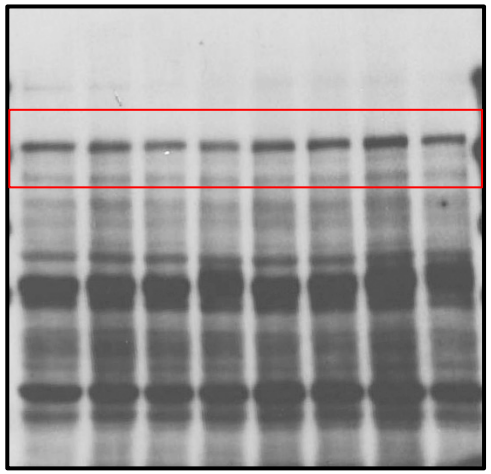

pERK5TEY

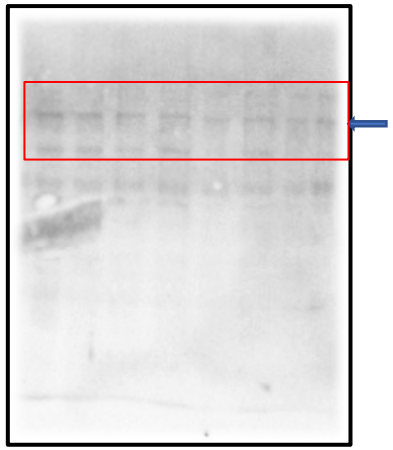

pERK5S496

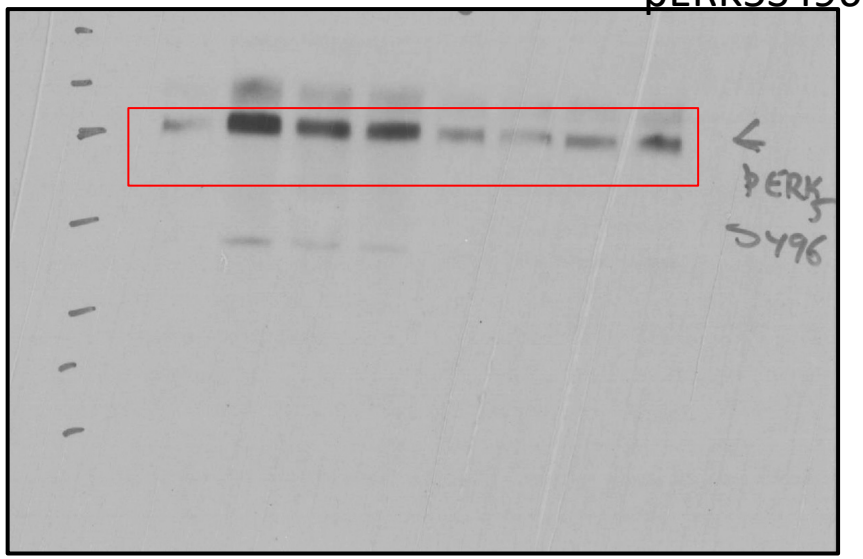

ERK5

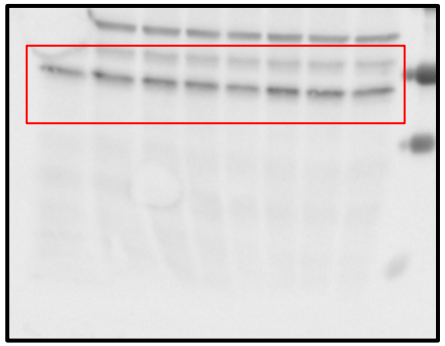

Figure 1H (Un-cropped)

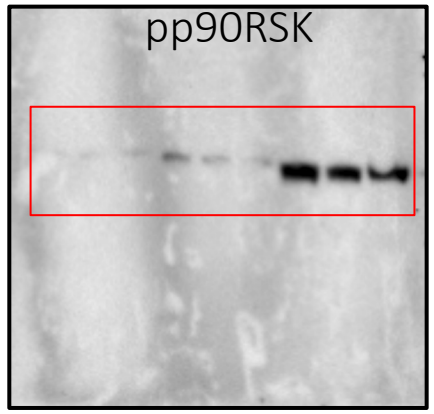

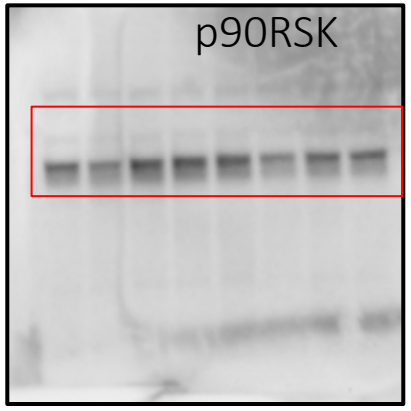

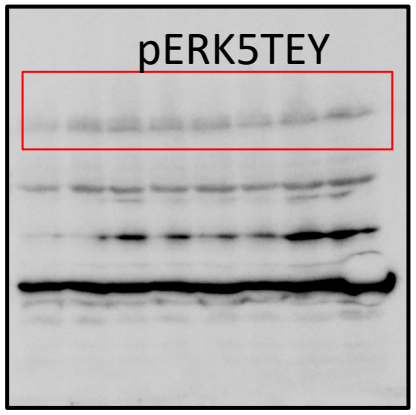

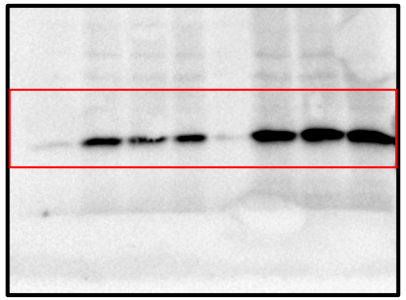

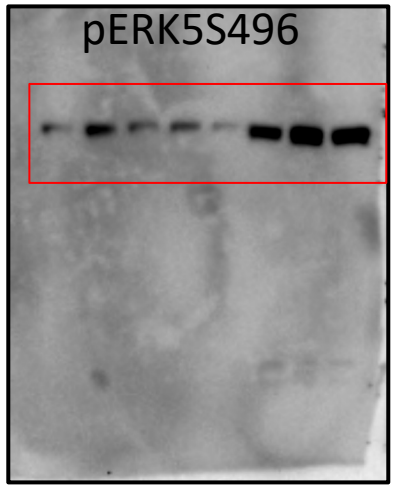

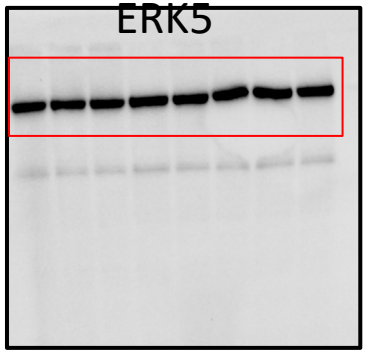

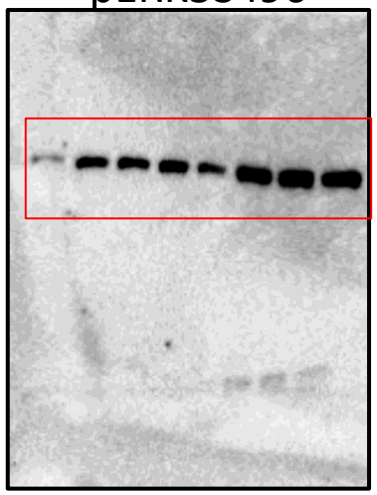

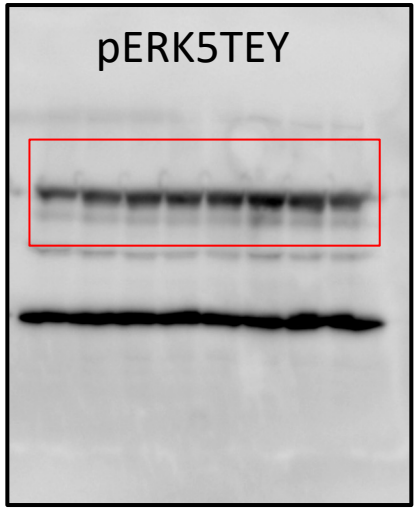

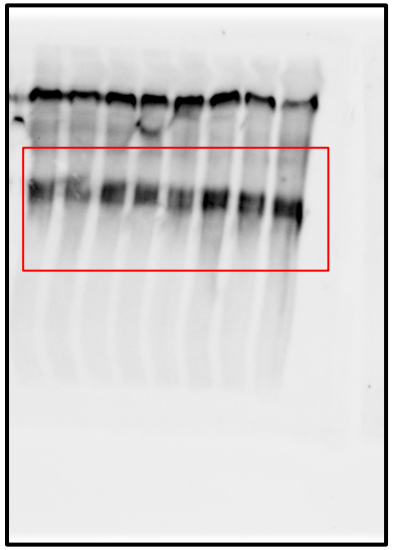

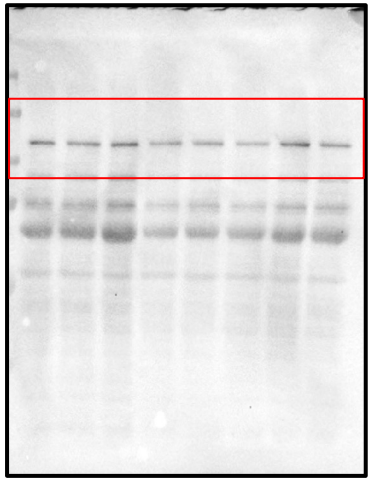

Figure 1I (Un-cropped)

HO1

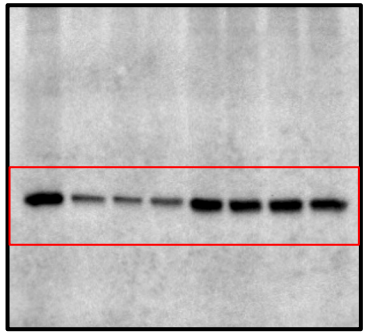

Trx1

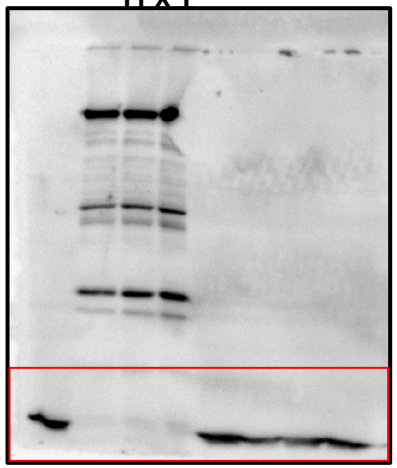

Gas6

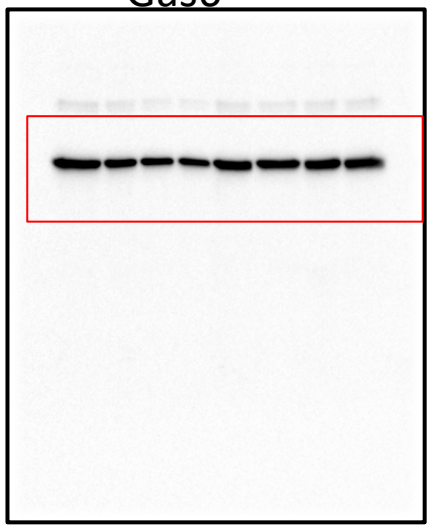

p53

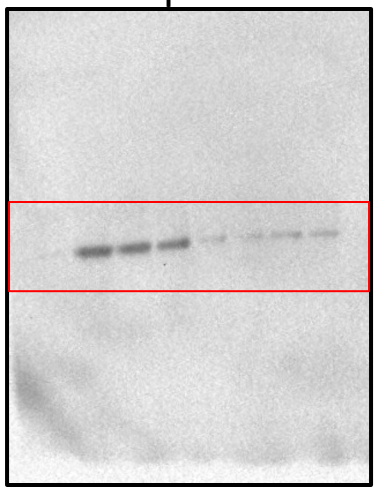

P53

p16

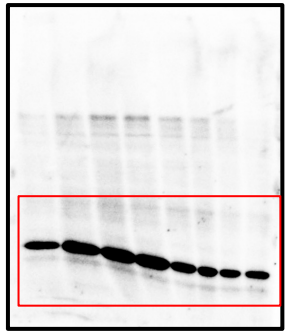

CD36

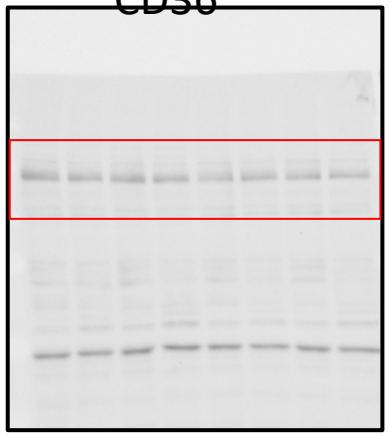

TNFA

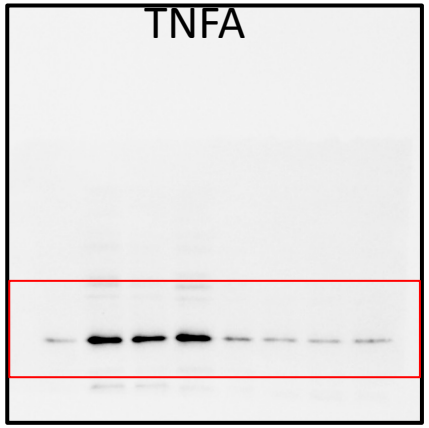

NRF2

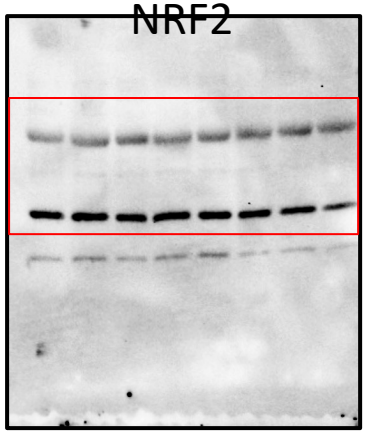

p21

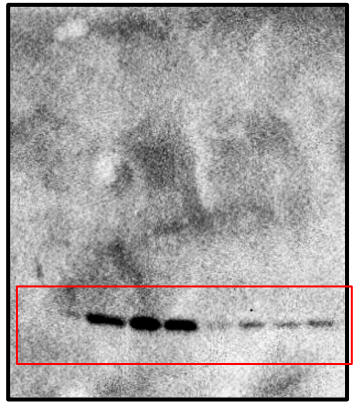

A-tubulin

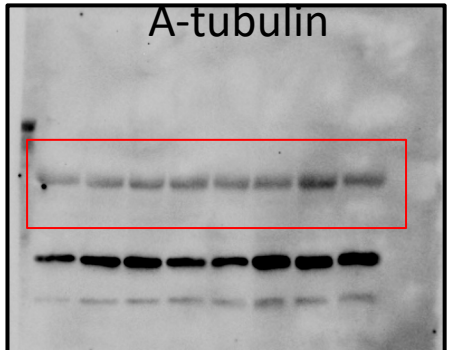

Figure 1N **(Un-cropped)**

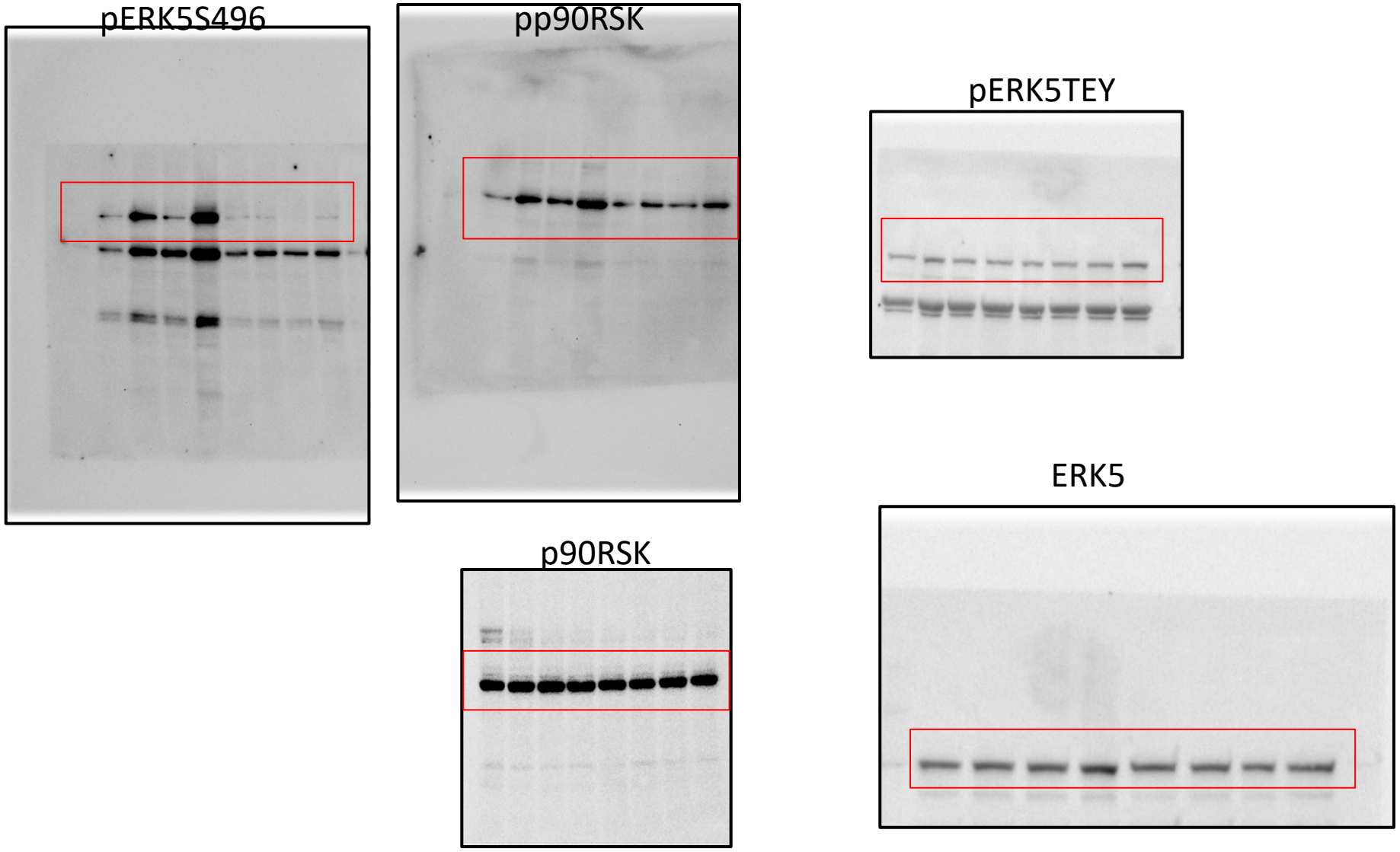

Figure 1N lower panel (Un-cropped)

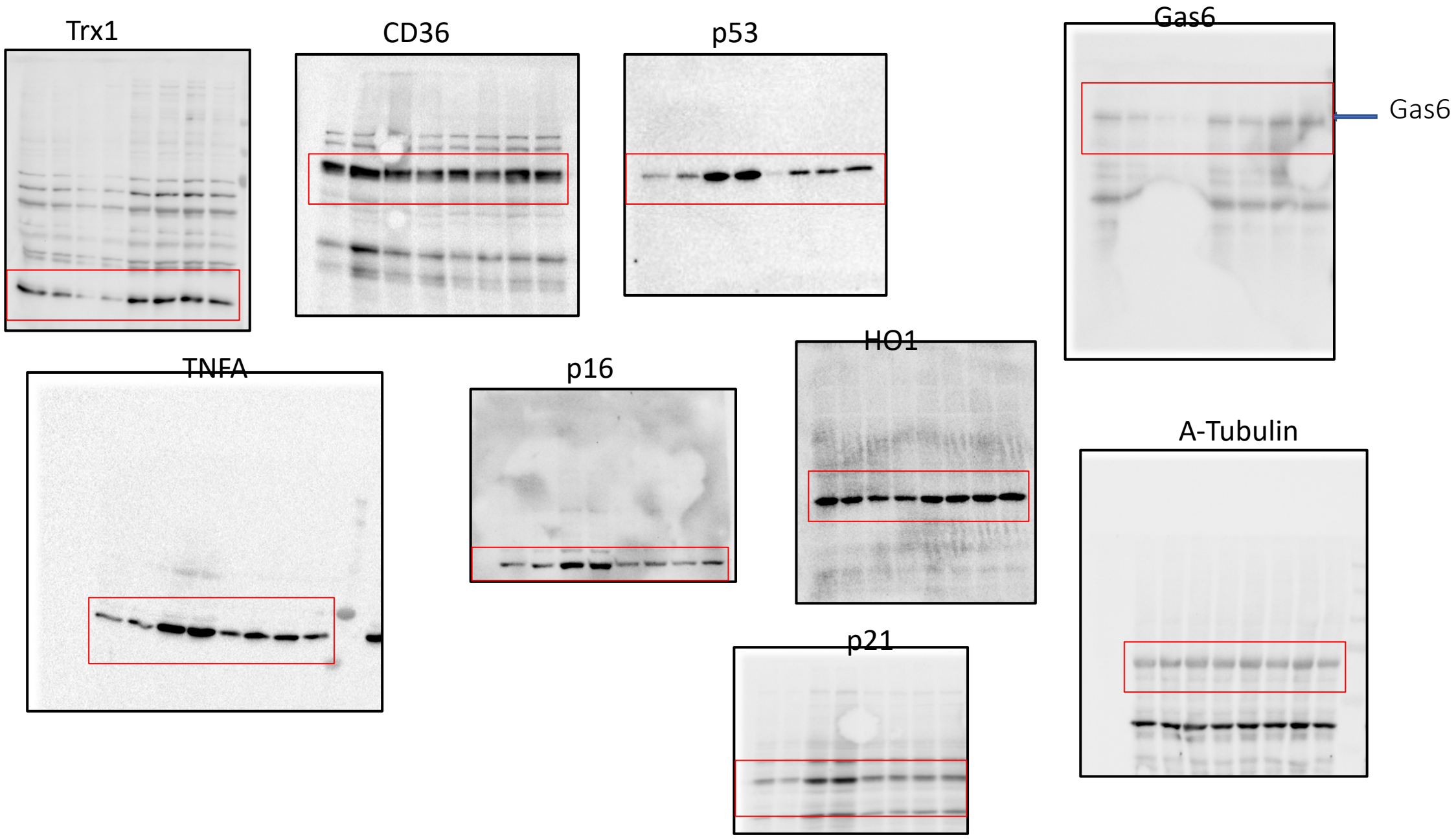

Figure 3A (Un-cropped)

pERK5S496

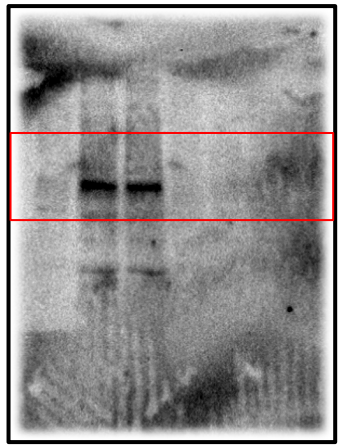

pERK5TEY

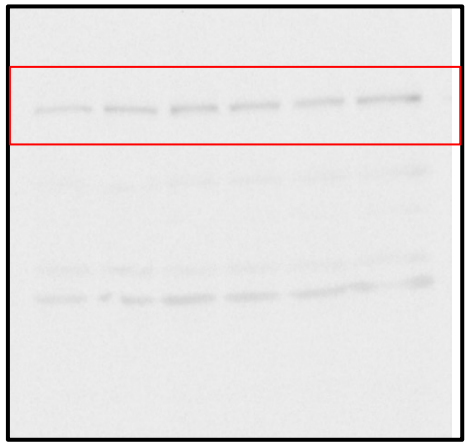

pp90RSK

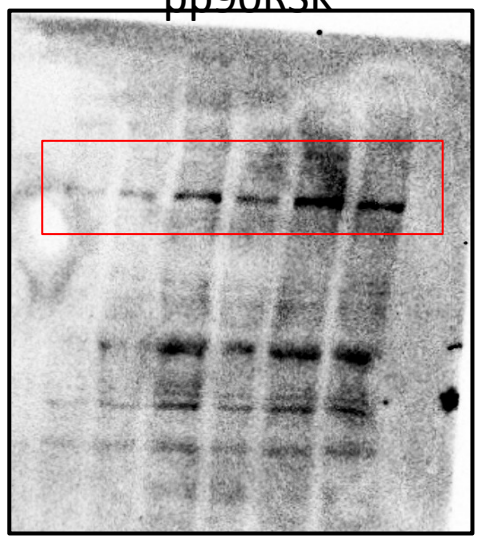

ERK5

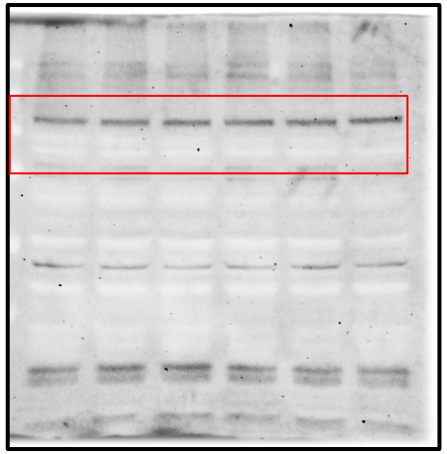

Figure 3D (Un-cropped)

p21

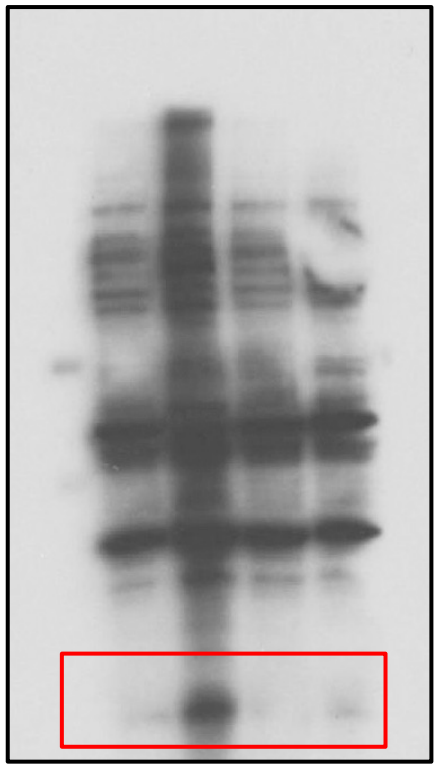

HO1

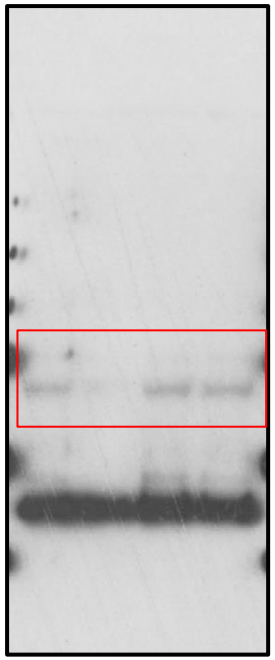

TRX1

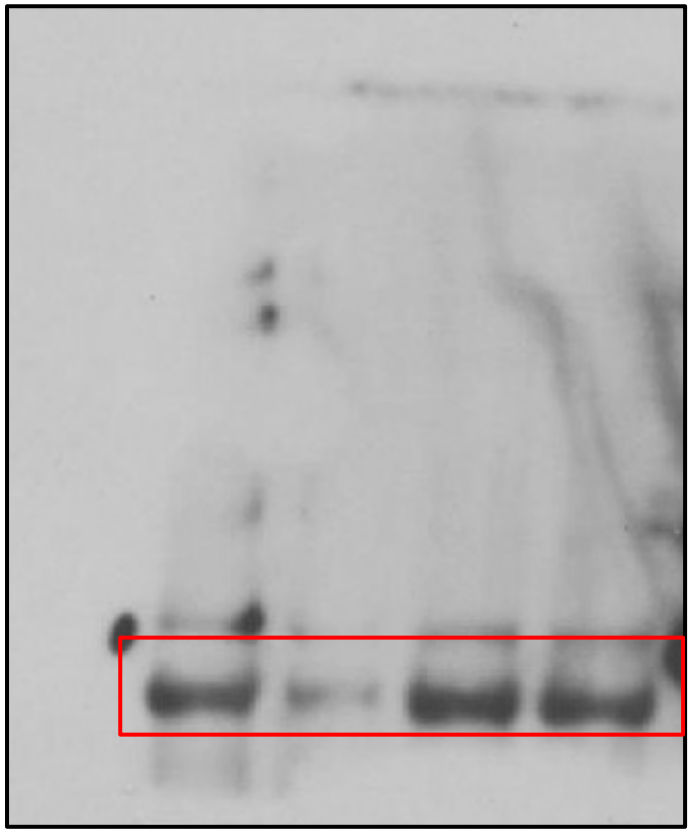

CD36

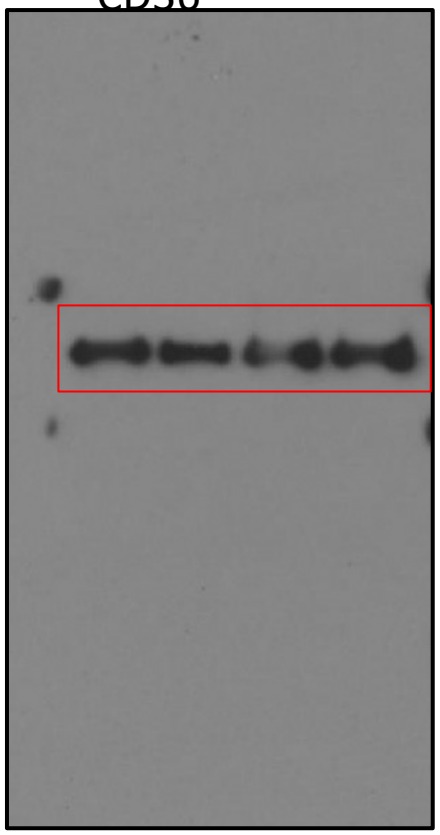

Figure 3D (Un-cropped)

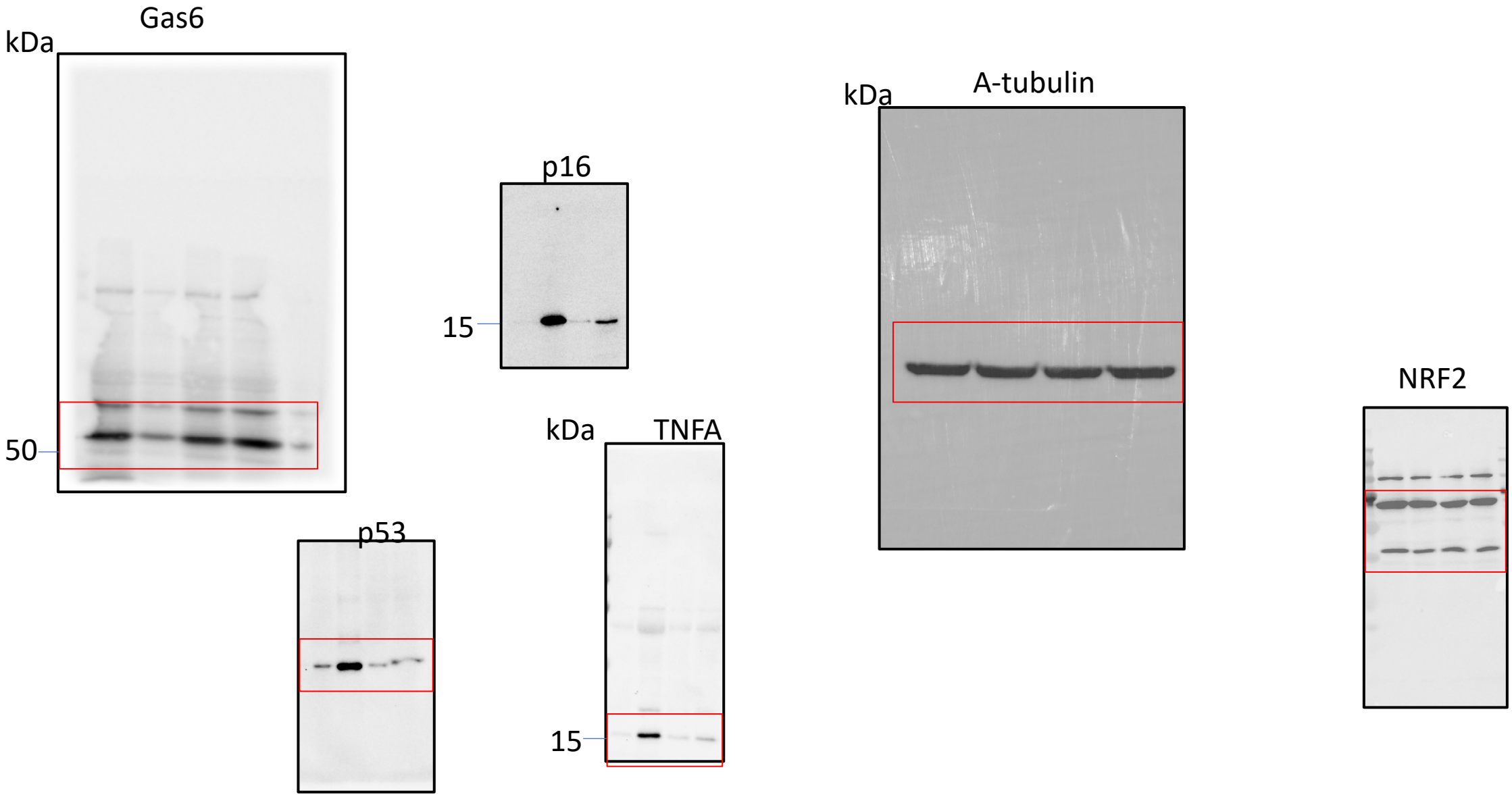

Figure 6A (Un-cropped)

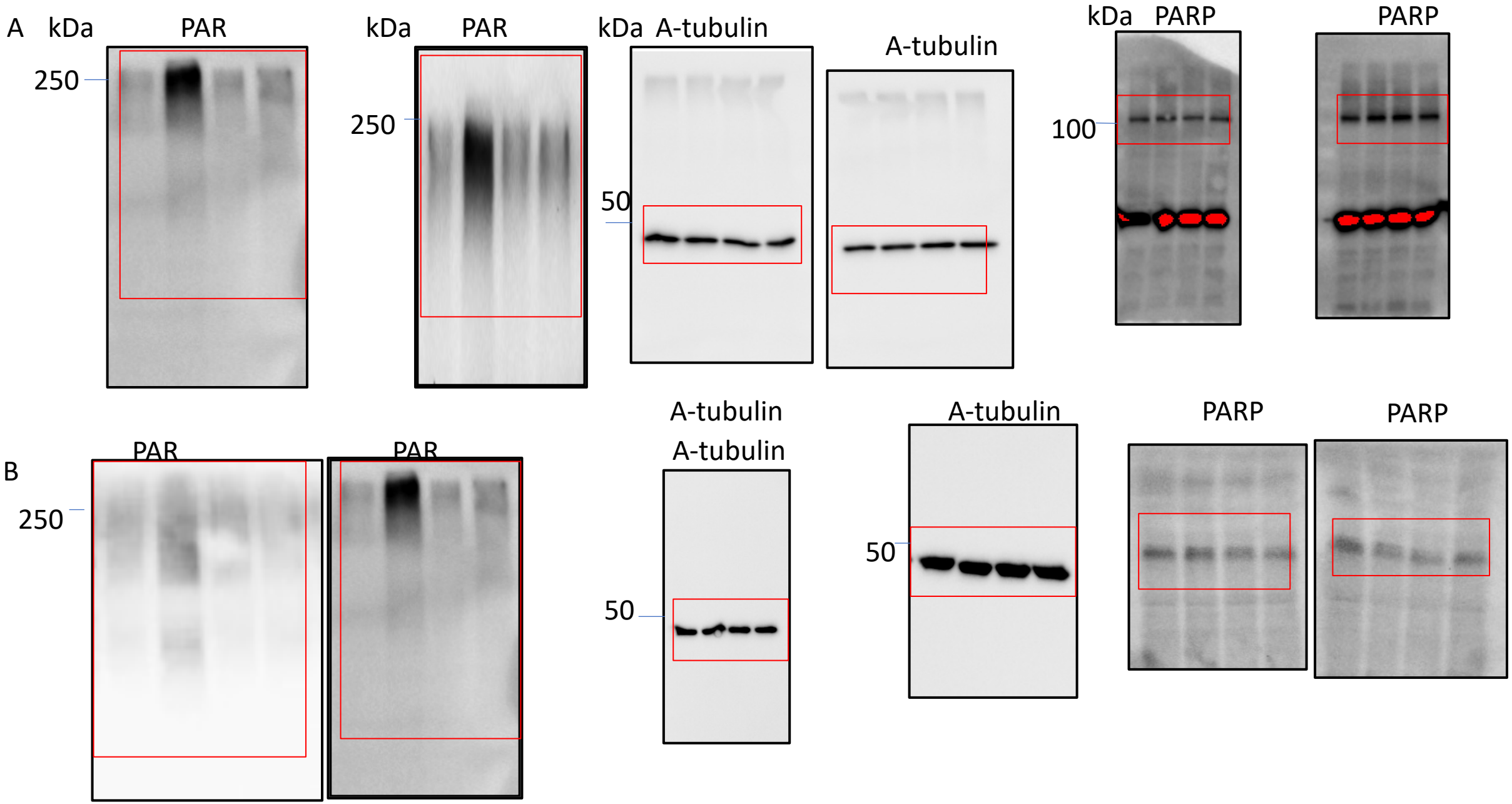

Figure 7H (Un-cropped)

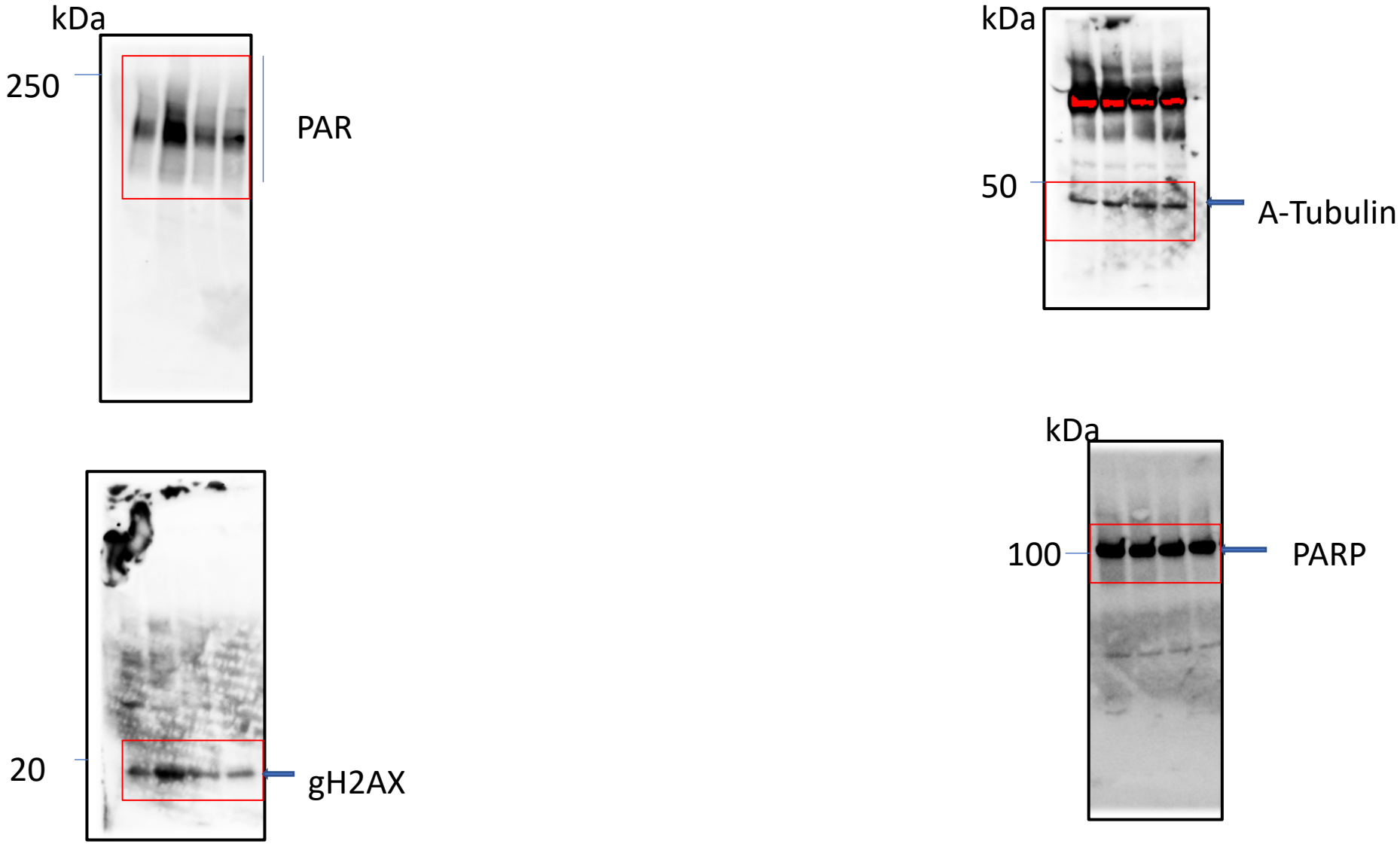

Suppl Figure 1C (Un-cropped)

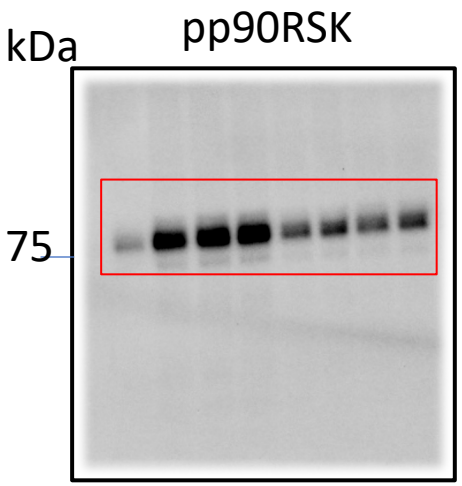

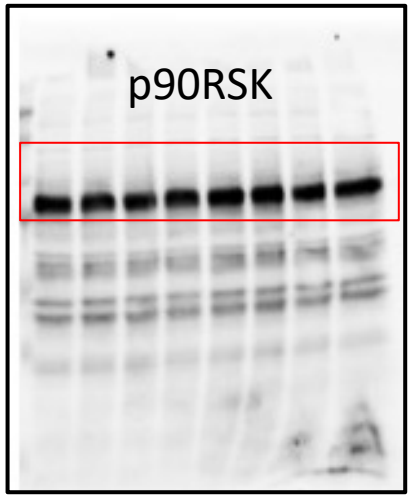

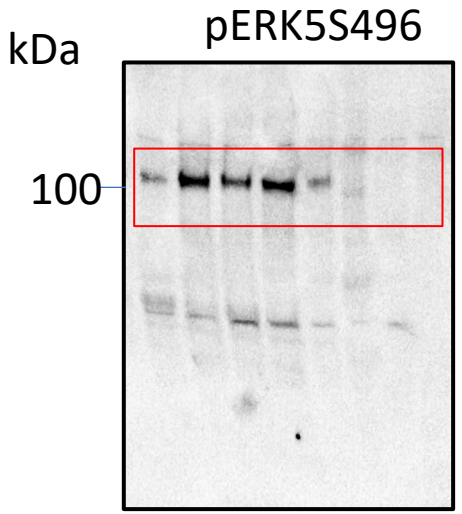

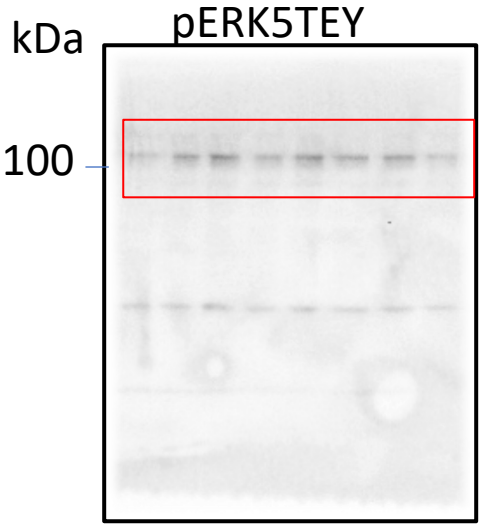

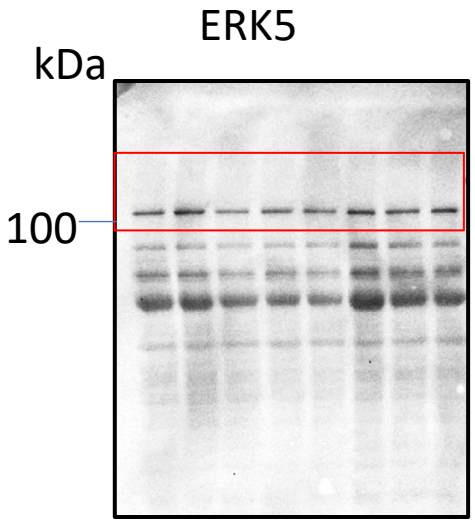

Suppl Fig 1E (Un-cropped)

HO1

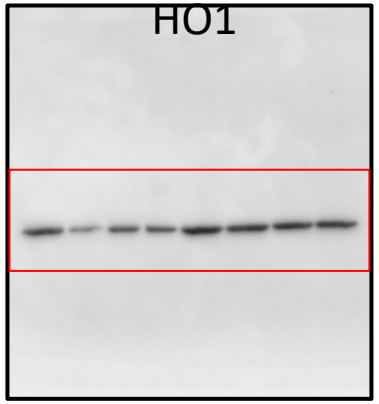

TNFA

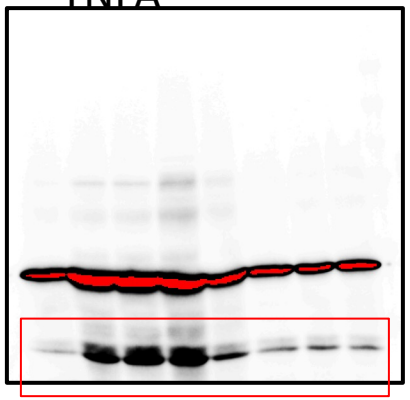

CD36

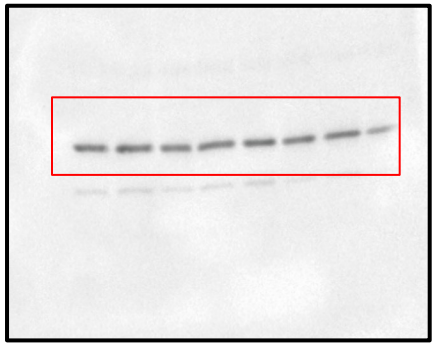

Gas6

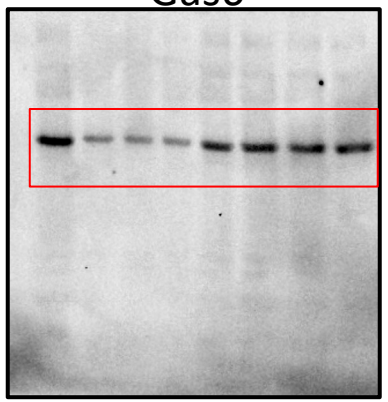

NRF2

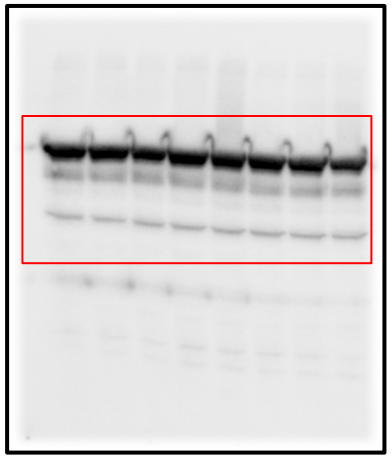

p16

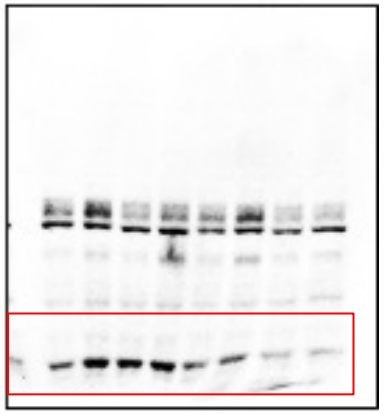

p53

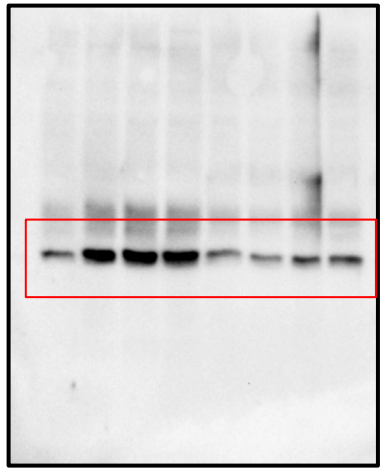

p21

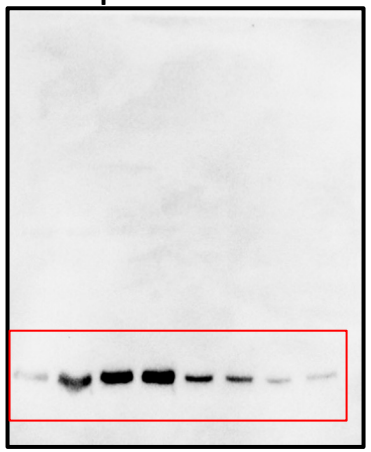

Trx1

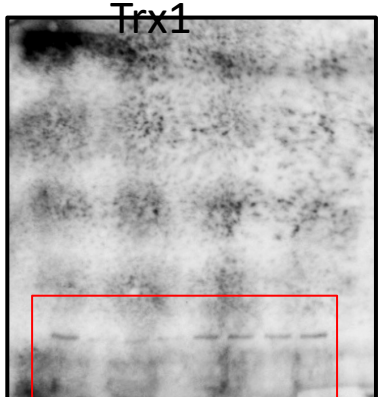

A-Tubulin

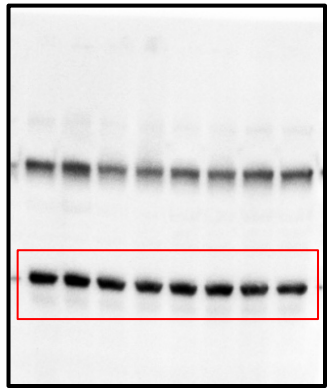

Sup figure 3 A, C (Un-cropped)

pP90rsk

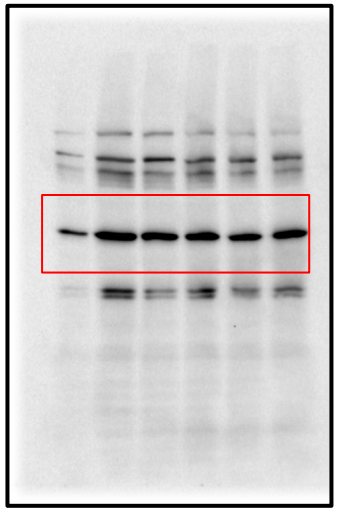

pERK5S496

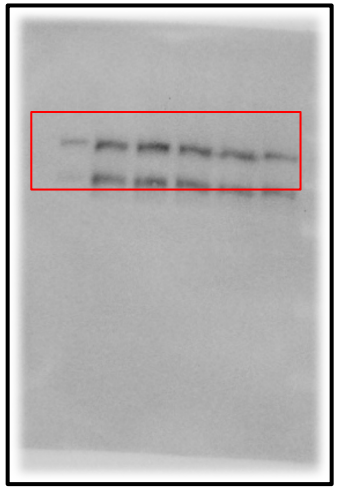

pERK5TEY

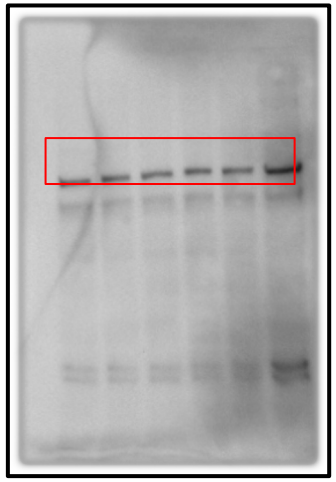

p90RSK

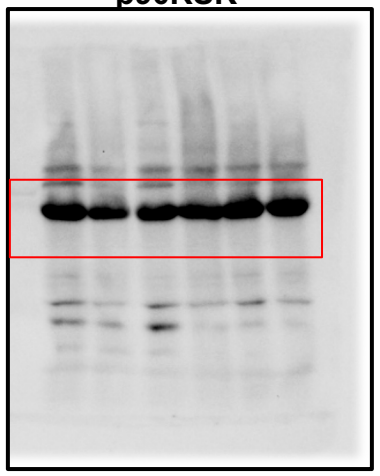

ERK5

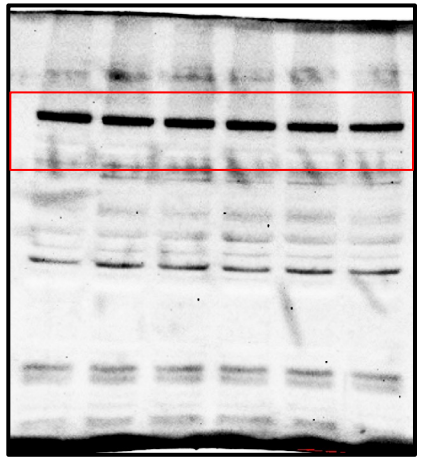

pP90rsk

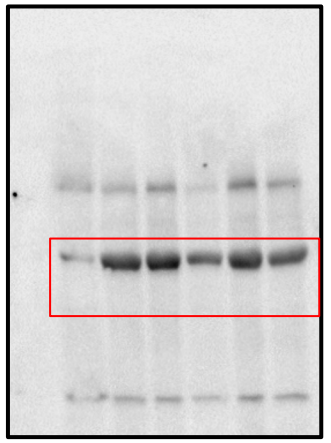

pERK5S496

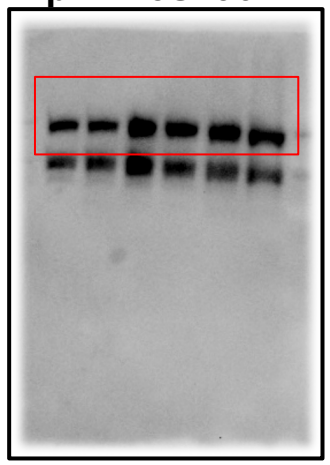

pERK5TEY

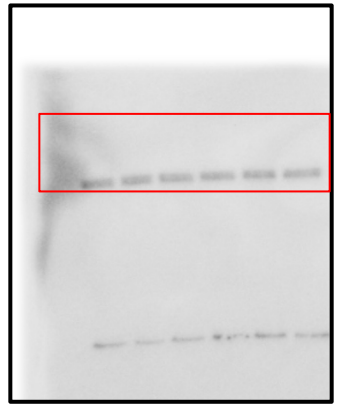

p90RSK

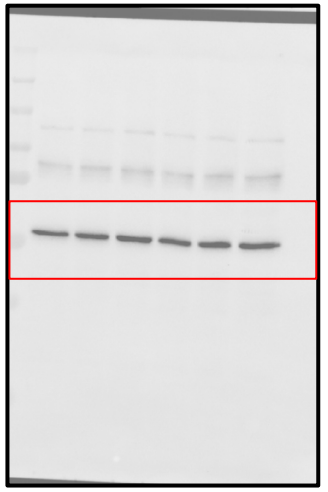

ERK5

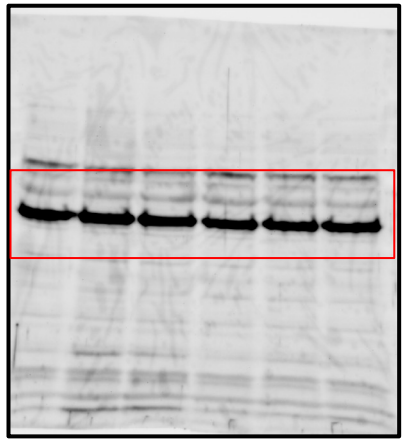

Sup figure 3F, H (Un-cropped)

pp90RSK

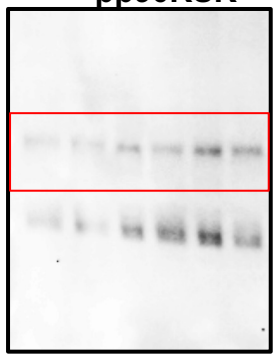

pERK5S496

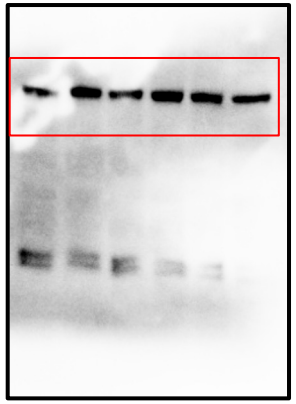

pERK5TEY

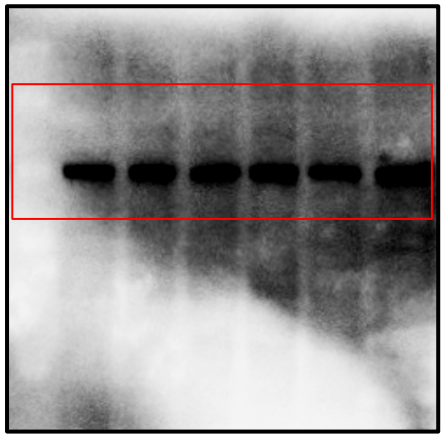

p90RSK

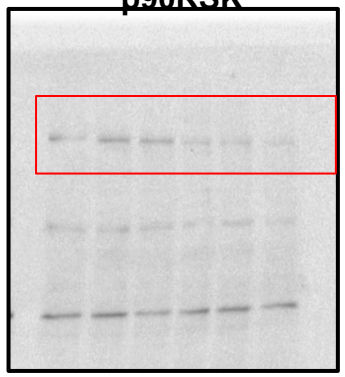

ERK5

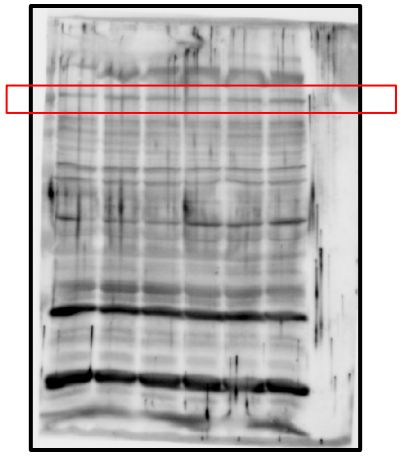

pp90RSK

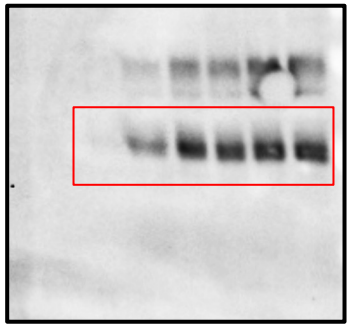

P90rsk

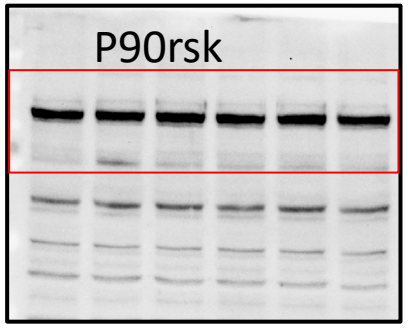

pERK5S496

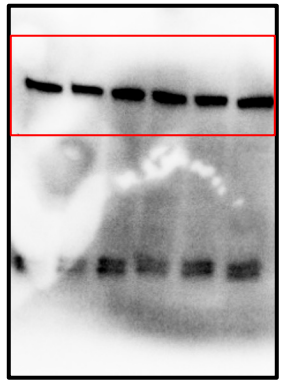

pERK5TEY

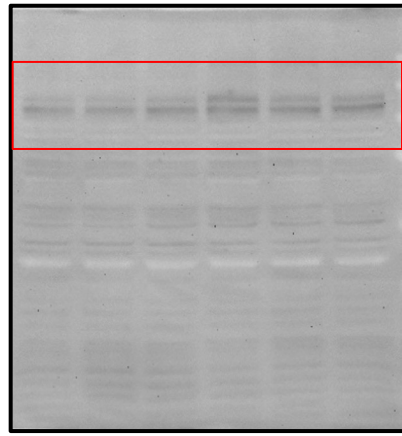

ERK5

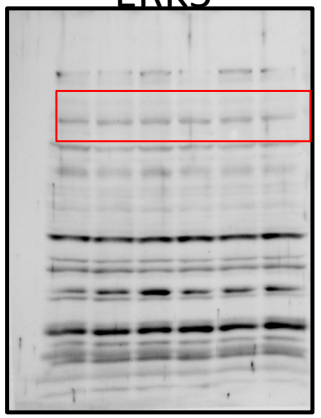

Sup figure 4A, C (Un-cropped)

pP90RSK

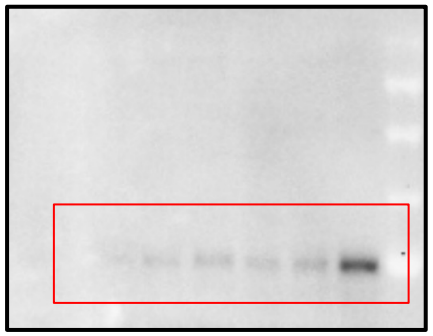

pERK5S496

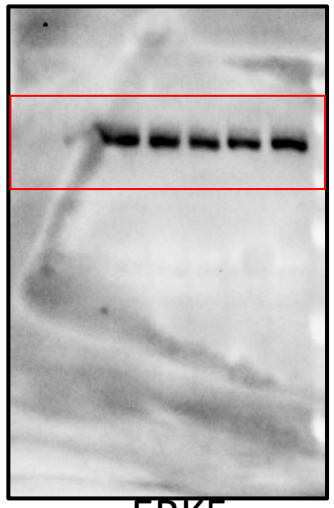

pERK5TEY

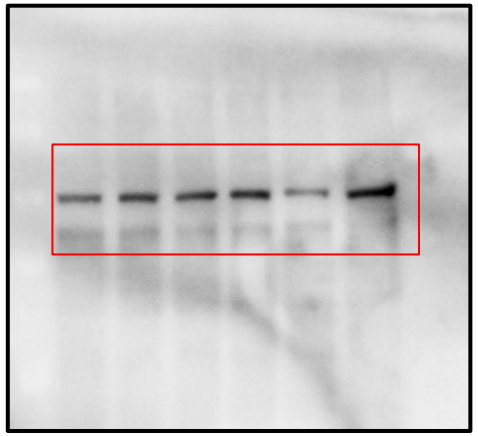

P90rsk

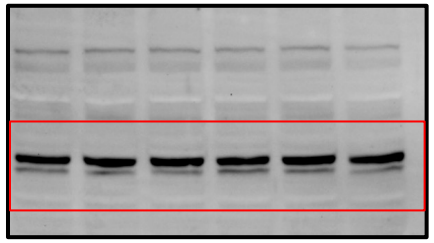

ERK5

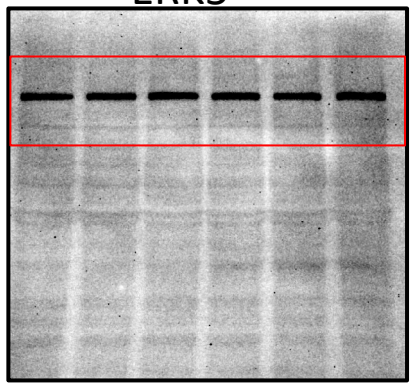

pP90rsk

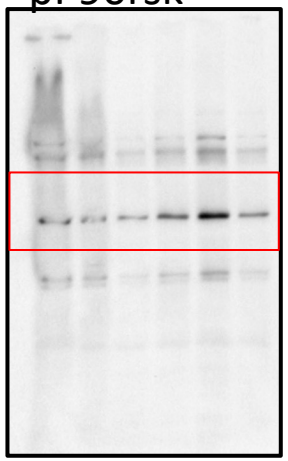

pERK5S496

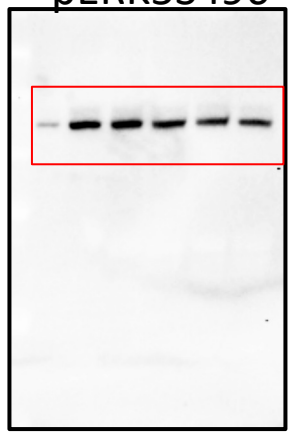

pERK5TEY

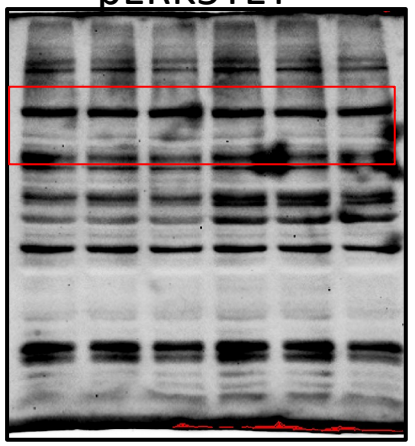

p90RSK

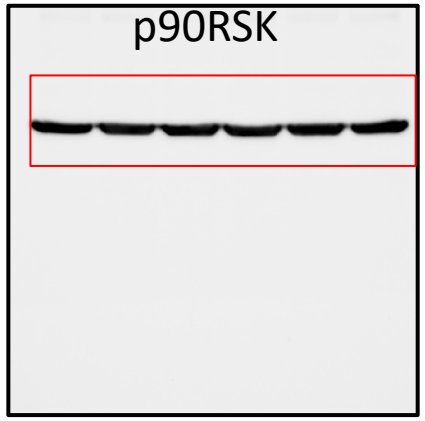

ERK5

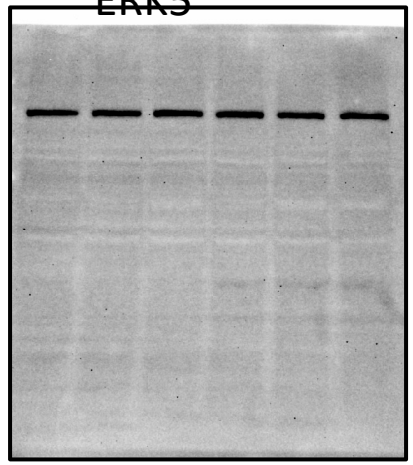

Sup figure 4F, H (Un-cropped)

pp90RSK

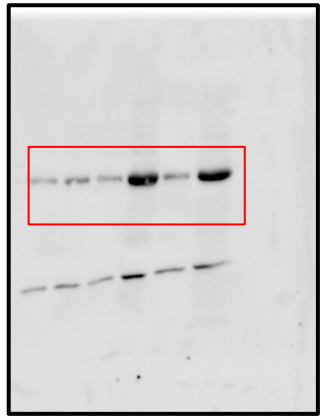

pERK5S496

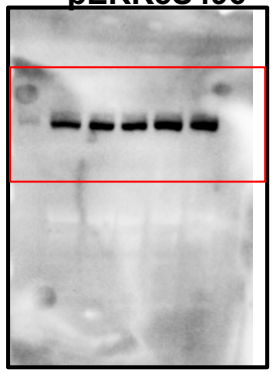

pERK5TEY

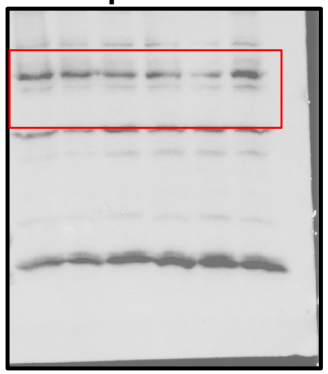

pp90RSK

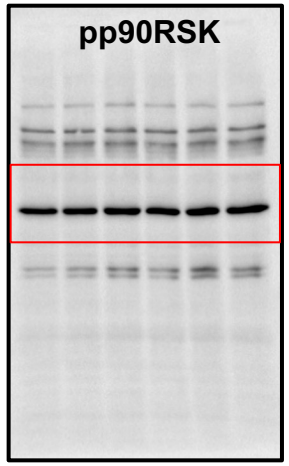

ERK5

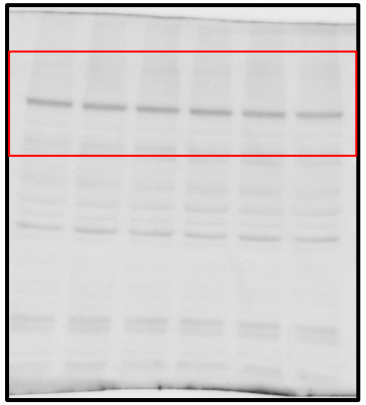

pp90RSK

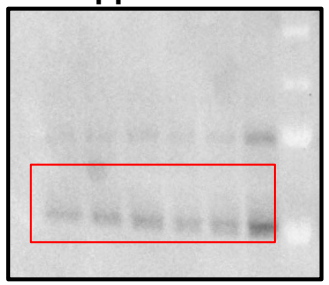

pERK5S496

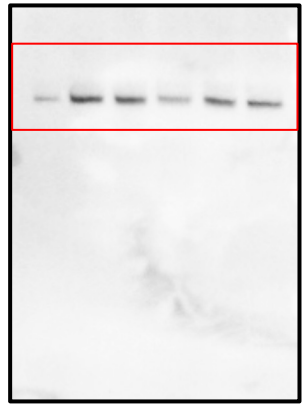

pERK5TEY

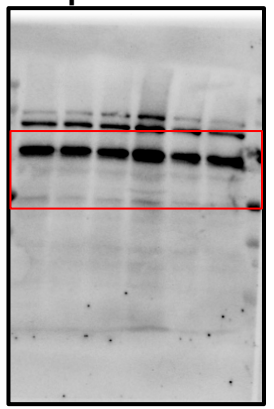

p90RSK

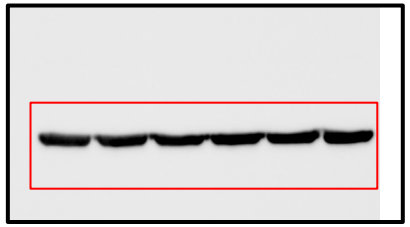

ERK5

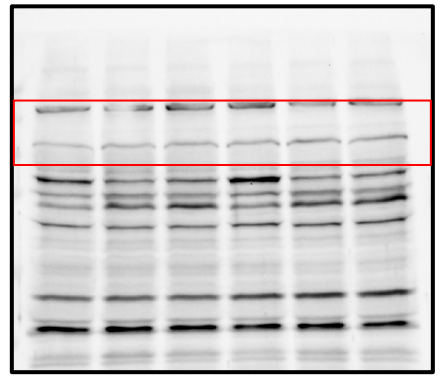

Suppl Figure 6 H (Un-cropped)

pp90RSK

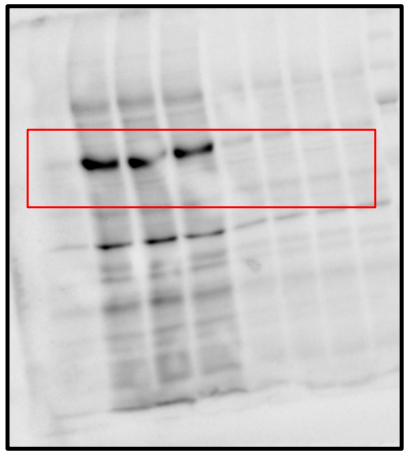

pERK5S496

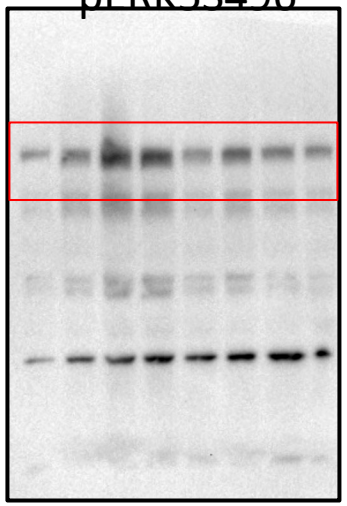

pERK5TEY

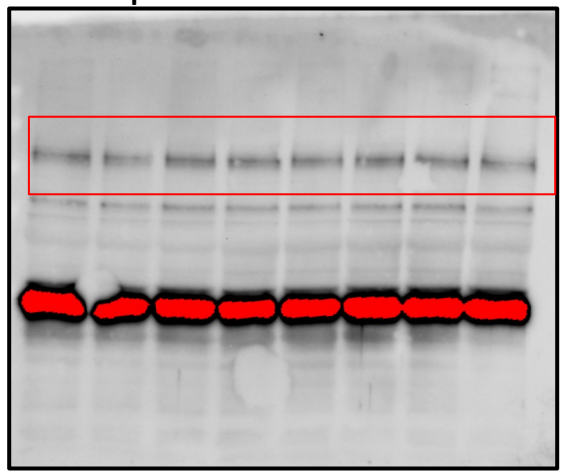

p90RSK

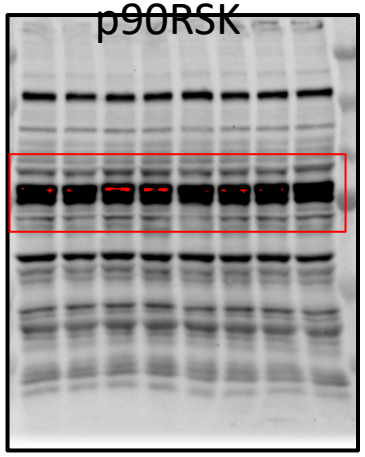

ERK55

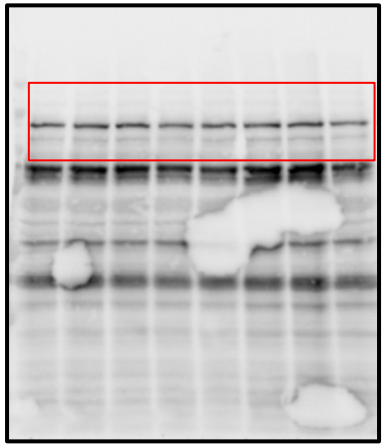

Suppl Figure 6 I (Un-cropped)